

Feature Article

Theory of dilute polyampholyte solutions in external electrical fields

Helmut Schiessel*, Alexander Blumen

Theoretical Polymer Physics, Freiburg University,
Rheinstr. 12, 79104 Freiburg, Germany

(Received: July 2, 1996; revised manuscript of July 17, 1996)

SUMMARY:

In this work we display recent findings on the conformations and dynamics of polyampholytes (PAs; polymers with positively and negatively charged monomers) in external electrical fields. We consider the case in which the interactions between the charges are less important (weak coupling limit) and also the case in which they are fundamental (strong coupling case). In the weak coupling limit we present analytical results for Gaussian and also for freely-jointed chains. Through scaling arguments we discuss the influence of the excluded volume on the PA's configurations. Furthermore we evaluate the dynamics of PAs in the framework of the Rouse and of the Zimm models. In the strong-coupling regime PAs with vanishing total charge form spherical globules. Using a droplet analogy we examine the response of PAs to external fields and show the onset of an instability reminiscent of a first-order phase transition.

1. Introduction

Recently polyampholytes (PAs), i.e. heteropolymers carrying quenched positive and negative charges along their backbone, have received much attention; the investigation of their conformational and dynamical properties is of much current interest. A characteristic feature of PAs are the competing interactions between the charged monomers. Thus PAs resemble in certain ways proteins, whose specific sequence of monomers induce their unique conformation^{1–5}. From a more general point of view PAs may be seen as being soft matter counterparts to random systems with competing interactions, such as spin glasses^{6,7}.

Many current investigations focus on the influence of the charge distribution on the PAs' conformational properties^{8–26}. For random PAs where the $\pm q$ charges are located randomly along the chain, the determination of the conformation is, however, a difficult task. The most important parameter here is the excess charge: Whereas neutral PAs form spherical globules¹², highly charged PAs behave similarly to polyelectrolytes, i.e., they are highly expanded. Theoretical and numerical investigations indicate a critical excess charge Q_c , namely $Q_c \approx q\sqrt{N}$ (N denotes the number of monomers), which marks the borderline between compact and expanded states^{17,20–22}. This is also consistent with experiments on polyampholyte solutions^{27–29} and gels^{30–33}, where both compact and extended conformations were observed.

Another question concerns the influence of an external electrical field on the dynamical and conformational properties of a PA with a given distribution of charges. Whereas the general situation is much more involved³⁴, in the weak coupling limit, i.e. when the interaction between the individual charges is of marginal importance, one has a generalized tug of war: the electric field acts on the charged monomers and pulls portions of the chain in different directions^{35–37}. A similar situation obtains for an A-B copolymer at the interface between two immiscible homopolymers A and B³⁸: the concentration profile perpendicular to the interface may exhibit an extended gradient region^{39,40}; if the A-B copolymer is located in this gradient region, its different monomers will feel forces in opposite directions, quite similar to the situation of a PA in an external electrical field.

Using analytical methods as well as scaling arguments we have calculated in a series of works^{34–37} the behavior of PAs in external electrical fields for different physical regimes. It is the purpose of this feature article to survey our present knowledge of the field and to make connections to related problems; by this we extend in several instances the previous approaches. In detail, the paper is organized as follows: In section 2 we discuss the role of the interactions between the charges. In section 2.1 we review following the lines of Higgs and Joanny¹² the results for neutral PAs (i.e. for which the overall charge vanishes); section 2.2 is devoted to the role of the excess charge for non-neutral PAs. Section 3 displays the conformational properties of PAs in external fields in the weak-coupling limit. Here we start by modeling the PA as a Gaussian chain in section 3.1, then as a freely-jointed chain in section 3.2 (cf. also ref.³⁷) and as an excluded volume chain in section 3.3³⁴. Section 4 is devoted to the conformational properties of a PA in the case when the interaction between the charges plays a dominant role (strong coupling); here an instability is predicted³⁴. In section 4 the dynamical properties of PAs in external fields are calculated in terms of the Rouse^{35,36} and of the Zimm dynamics. Our conclusions are summarized in section 5.

2. Randomly charged PAs: collapsed and stretched conformations

Two antagonistic effects determine the overall shape of a PA. First the Coulomb attraction of oppositely charged monomers may induce a collapse. Secondly, the PA may have an excess charge; this leads to a repulsion which may induce a stretching of the chain. In order to distinguish between these two mechanisms we first report in section 2.1 some results for neutral PAs, whereas the influence of an excess charge is discussed in section 2.2.

2.1. Collapse of neutral chains

Consider a PA with zero total charge, whose polymerisation degree is N , $N \gg 1$. A fraction $2f$ of the monomers is charged, so that one has fN positive charges $+q$ and fN negative charges $-q$. The charges are distributed randomly along the chain and form a quenched pattern. We assume furthermore that no counterions are present;

such counterions are not required experimentally since the PAs are — as a whole — already neutral. As it is well-known^[2, 22] such neutral PAs collapse to spherical globules with a volume V significantly smaller than the unperturbed chain volume $b^3N^{3\nu}$ and significantly larger than the volume b^3N of the closely packed configuration. Here b denotes the monomer size and the Flory exponent ν equals $3/5$ for a swollen chain (good solvent) and $1/2$ for an ideal chain (θ -solvent). Thus the following relations hold:

$$b^3N \ll V \ll b^3N^{3\nu} \quad (1)$$

which impose some restrictions on the physical parameter (see below). Edwards, King and Pincus^[8] suggested that a neutral PA behaves similarly to a (micro)electrolyte confined to a volume V . Starting from this assumption Higgs and Joanny^[12] estimated the volume of such a PA using the Debye-Hückel approximation (see also ref.^[17]). Neglecting the connectivity of the chain the *screening length* r_D within the PA can be estimated as in the case of an electrolyte: In the volume r_D^3 there is a typical excess charge of the order $\sqrt{f\rho r_D^3}q$, with $\rho = N/V$ being the density of monomers. Letting the electrostatic interaction between such volumes be at most of the thermal energy T (expressed in units of the Boltzmann constant k_B) leads to the condition $(f\rho r_D^3)q^2/(\epsilon r_D) \approx T$ (where ϵ denotes the dielectric constant of the solvent). Thus one finds $r_D = \sqrt{V/(fNl_B)}$, with $l_B = q^2/(\epsilon T)$ being the *Bjerrum length*. At length scales shorter than r_D the thermal fluctuations dominate and the interaction between the monomers can be neglected. At length scales comparable to r_D the monomers will arrange themselves such that monomer groups which have a positive excess charge are surrounded by groups with negative excess charge, and vice versa (screening). Thus one finds for the electrostatic free energy of densely packed groups $F_e \approx -(V/r_D^3)T$, which is the classical result of the Debye-Hückel approximation^[41]:

$$\frac{F_e}{T} \approx -\frac{fNl_B}{r_D} = -\frac{(fNl_B)^{3/2}}{V^{1/2}} \quad (2)$$

(In Eq. (2) and in other similar expressions of this section we omit dimensionless constants of order unity.)

The electrostatic part of the free energy, Eq. (2), induces a collapse; the size of the PA will be lowered until the monomers' excluded volume balances the attractive forces^[12]. The contribution F_1 of the excluded volume to the free energy of a polymer confined inside a volume V can be estimated using scaling arguments as follows^[42, 43]: The osmotic pressure $\Pi = -\partial F_1/\partial V$ has the form $\Pi = (T\rho/N)f(\rho/\rho^*)$ where f is a scaling function and ρ^* is the critical monomer density at which the polymer occupies the whole volume, i.e., $\rho^* \approx N/(b^3N^{3\nu})$. For $\rho \ll \rho^*$ (small concentrations) f is a constant and one recovers the ideal gas law. In the semi-dilute regime ($\rho^* \ll \rho \ll b^{-3}$) which we are interested in, Π has to be a function of ρ only and has to be independent of N . This requirement leads to $f(x) \propto x^m$ with $m = 1/(3\nu - 1)$. Thus $\Pi \approx Tb^{3/(3\nu-1)}\rho^{3\nu/(3\nu-1)}$ from which F_1 follows by integration:

$$\frac{F_1}{T} \approx \frac{b^{3/(3\nu-1)} N^{3\nu/(3\nu-1)}}{V^{1/(3\nu-1)}} \quad (3)$$

Note that for the θ -case ($\nu = 1/2$) F_1 represents the three-body collision term, i. e., $F_1 \approx b^6 N^3 / V^2$. Minimizing $F = F_e + F_1$ with respect to V , Higgs and Joanny¹²⁾ find that

$$V \approx b^3 N \left(\frac{b}{f l_B} \right)^{(3\nu-1)/(1-\nu)} = \begin{cases} b^3 N \frac{b}{f l_B} & \text{for } \nu = 1/2 \text{ (ideal chain)} \\ b^3 N \left(\frac{b}{f l_B} \right)^2 & \text{for } \nu = 3/5 \text{ (swollen chain)} \end{cases} \quad (4)$$

Thus this Flory-type argument predicts a collapsed PA globule with a monomer density of $\rho \approx f l_B / b^4$ in a θ -solvent and of $\rho \approx (f l_B)^2 / b^5$ in a good solvent. Note, however, that the argument used is only valid as long as the PA's volume, Eq. (4), lies within the interval given by Eq. (1). This leads to the following condition:

$$f l_B \ll b \ll N^{1-\nu} f l_B \quad (5)$$

The first inequality is necessary for the Debye-Hückel approximation to hold⁴¹⁾, the second one means that the electrostatic interaction overcomes the thermal agitation of the chain (strong-coupling case). In the opposite case

$$b > N^{1-\nu} f l_B \quad (6)$$

the electrostatic interaction between the charges is less than the thermal effects (weak-coupling case) and the PA has the usual Gaussian (θ -solvent) or excluded volume (good solvent) conformation. In this *weak coupling limit* the behavior of a PA in external electrical fields can be treated analytically³⁵⁻³⁷⁾ (see section 3 for statistical and section 5 for dynamical features). Condition (6) can be attained readily by taking a solvent with a large dielectric constant: one has for water at room temperature $l_B \cong 7 \text{ \AA}$ so that for small f Eq. (6) is readily fulfilled.

The strong-coupling case, i. e. when Eq. (5) is obeyed, can be visualized in terms of the following blob picture¹²⁾: The electrostatic free energy is comparable to T for subchains of size $r \approx r_D$ (cf. Eq. (2)). These *Debye blobs* obey $r \approx r_D \approx b g_D^\nu$, where g_D is the number of monomers per blob. This, together with $r_D \approx f g_D l_B$ gives $g_D \approx (b/f l_B)^{1/(1-\nu)}$. By assuming that the whole PA is densely packed with swollen (ideal) blobs, the volume of the PA is estimated as being $V \approx (N/g_D) r^3$, from which Eq. (4) again follows.

Victor and Imbert¹⁶⁾ and Wittmer, Johner and Joanny¹⁸⁾ considered also PAs where the positive and negative charges are placed in an alternating fashion. They showed that the Debye-Hückel approximation is inapplicable to such PAs. An alternating PA undergoes a collapse transition similar to that displayed by an uncharged polymer in a poor solvent; furthermore the collapsed chain behaves as a dielectric material (cf. also the experimental study by Neyret et al.⁴⁴⁾). Another type of a non-random arrangement of charges, for which the Debye-Hückel treatment has been refined, is given by the symmetric diblock PA¹⁰⁾ where one half of the chain contains positively charged, the other half negatively charged monomers.

2.2 Effect of a net charge

The Debye-Hückel argument given above is based on the strict electroneutrality of the system. The collapse mechanism of neutral PAs stems from the screening of the charges and does not hold for highly charged chains; for these the repelling force of the unscreenable excess charge Q_{tot} induces the stretching of the chain. Comparing the size of a Debye blob with the polyelectrolyte blob size Higgs and Joanny¹²⁾ conclude that a PA with a sufficiently high net charge stretches out in a way similar to a polyelectrolyte⁴⁵⁾. In another approach (which is analogous to the renormalization treatment for polyelectrolytes⁴⁶⁾) Kantor and Kardar¹¹⁾ find that due to typical charge fluctuations of order $q\sqrt{fN}$ the PA extends.

An important improvement in the understanding of the behavior of charged PAs is the realization that the surface tension of the globular state may play a dominant role. For a PA whose net charge exceeds a certain critical value Gutin and Shakhnovich¹⁹⁾ predict the elongation of the globule due to the competition between surface tension and the electrostatic repulsion. They find this effect to be drastic for PAs whose charge sequences are correlated over long ranges (such sequences have been found, for instance, in DNA⁴⁷⁾). Using a two-parameter Flory theory Dobrynin and Rubinstein²¹⁾ conclude that PAs with sufficiently high charge asymmetry show three characteristic regimes: at high temperatures there is a region where the charges are unimportant (unperturbed regime); this is followed at intermediate temperatures by a polyelectrolyte-type regime in which the chain is stretched into a string of blobs. At sufficiently small temperatures, however, the fluctuation induced attraction dominates and one finds²¹⁾ an elongated globule, similar to ref.¹⁹⁾. We note that these scaling approaches are focused on the overall shape of the elongated globule, i.e. its length and width. In refs.^{20, 22)} Kantor and Kardar suggest that, in analogy to charged drops, a more refined analysis is needed; they conclude that the PA may stretch out in a necklace shape. The inhomogeneities of the charge distribution may perturb the geometry of an ordered necklace; thus a detailed study of the properties of the charge distribution is necessary²⁵⁾.

The critical value of the excess charge Q_{tot} which separates the regimes of stretched PAs from collapsed PAs can be roughly estimated by the following argument given by Kantor and Kardar²²⁾: Denote the charge of the n th bead by q_n ($n = 0, 1, \dots, N - 1$) and take it to be a quenched variable (i.e. the set $\{q_n\}$ stays fixed for a given PA). Q_{tot} is evidently $Q_{tot} = \sum_n q_n$. Consider now for fixed Q_{tot} the random $\{q_n\}$ sets involved. Here each monomer is taken to be either positively or negatively charged, i.e. $q_k = \pm q$. Thus out of N monomers N_+ carry the charge $+q$ and N_- monomers the charge $-q$; one has $N = N_+ + N_-$ and $N_+ - N_- = Q_{tot}/q$. For a random distribution of such charges along the chain one has the following charge correlations:

$$\langle q_i q_j \rangle = \begin{cases} q^2 & \text{for } i = j \\ \frac{Q_{tot}^2 - q^2 N}{N(N-1)} & \text{for } i \neq j \end{cases} \quad (7)$$

Here the brackets $\langle \dots \rangle$ denote averages with respect to different realizations of the $\{q_n\}$ sequences. At sufficiently high temperatures the geometry of the PA is only slightly perturbed and the PAs' radius of gyration obeys $R_g \sim N^\nu$. Using Eq. (7) and taking R_g as a measure for the typical interparticle distances one finds for the electrostatic energy

$$\overline{\langle U_e \rangle} \approx \varepsilon^{-1} \sum_{i \neq j} \langle q_i q_j \rangle \overline{1/|r_i - r_j|} \approx \frac{Q_{tot}^2 - q^2 N}{\varepsilon R_g} \quad (8)$$

where the thermal average is denoted by the dash, $\overline{\dots}$. We note in Eq. (8) the appearance of a critical charge $Q_c \equiv q \sqrt{N}$ connected with a change of sign for $\overline{\langle U_e \rangle}$ as a function of Q_{tot} . We define now $T_{Q_{tot}} \approx |\overline{\langle U_e \rangle}|$. For $T \gg T_{Q_{tot}}$ the electrostatic interaction plays a minor role. Decreasing T below $T_{Q_{tot}}$ the electrostatic interaction induces a change of the PAs conformation: PAs with $Q_{tot} < Q_c$ will lower $\overline{\langle U_e \rangle}$ by shrinking with decreasing temperature whereas chains with $Q_{tot} > Q_c$ will expand when T is lowered. Note that for $Q_{tot} = 0$ the condition for the unperturbed state, $b > N^{1-\nu} l_B$ (cf. Eq. (6)), is indeed equivalent to the condition $T_{Q_{tot}=0} > |\overline{\langle U_e \rangle}|$. Numerical simulations of PAs confirm these arguments²²⁾.

The \sqrt{N} -dependence of the critical excess charge Q_c has interesting consequences for random PAs where the charges are distributed uncorrelated along the chain, i.e., where the charge correlations obey

$$\langle q_i q_j \rangle = q^2 \delta_{ij} \quad (9)$$

This implies automatically that the average of the total charge vanishes, i.e., $\langle Q_{tot} \rangle = 0$. A given chain, however, is not necessarily neutral and the mean-squared total charge is given by $\langle Q_{tot}^2 \rangle = q^2 N$ which is of same order as Q_c^2 . Thus for a given ensemble of random PAs one may find compact globules as well as highly stretched configurations.

3. Conformational properties of PAs in external fields (weak coupling limit)

This section is devoted to the equilibrium properties of single polyampholyte chains when the electrostatic interaction between charges can be neglected, i.e. when condition Eq. (6) is fulfilled. In this weak coupling limit and in the absence of an external electrical field the chain is practically unperturbed so that the PA takes the conformation of a Gaussian or an excluded volume coil depending on the solvent's quality.

3.1. Gaussian chain

Here we are interested in the linear response of PAs to electrical fields; this implies that the external fields and thus the deformations are not too large. In this subsection we assume the θ -condition and thus neglect the excluded volume effect. We relegate the discussion of the finite chain's extensibility under large deformations to subsection 3.2 and consider swollen PAs in subsection 3.3.

We view the PA as a Gaussian chain, i.e. as consisting of N charged beads, connected into a linear chain by harmonic springs. The chain's position is given by the set $\{\mathbf{R}_n\}$, where $\mathbf{R}_n = (X_n, Y_n, Z_n)$ is the position vector of the n th bead ($n = 0, 1, \dots, N-1$). In the absence of intramolecular electrostatic and of excluded volume interactions the potential energy $U(\{\mathbf{R}_n\})$ of the PA chain contains only the elastic contributions of the neighbouring segments and the interactions with the external electric field \mathbf{E} :

$$U(\{\mathbf{R}_n\}) = \frac{K}{2} \sum_{n=1}^{N-1} [\mathbf{R}_n - \mathbf{R}_{n-1}]^2 - \mathbf{E} \sum_{n=0}^{N-1} q_n \mathbf{R}_n - f(\mathbf{R}_i - \mathbf{R}_j) \quad (10)$$

In Eq. (10) K denotes the spring constant $K = 3T/b^2$. The third term is introduced mainly for technical reasons: it can be used (see below) to derive readily from the partition function the average distance between the i th and the j th monomer with $0 \leq j < i \leq N-1$. Alternatively the chain's configuration can be represented by the set $\{\mathbf{r}_n\}$ of bond vectors $\mathbf{r}_n = \mathbf{R}_n - \mathbf{R}_{n-1}$ ($n = 1, \dots, N-1$) from which the positions of the beads follow:

$$\mathbf{R}_n = \mathbf{R}_0 + \sum_{k=1}^n \mathbf{r}_k \quad (11)$$

Introducing further the cumulative charge variable $Q_k = \sum_{j=k}^{N-1} q_j$, the potential energy, Eq. (10), can be reformulated as:

$$\begin{aligned} U(\{\mathbf{r}_n\}) = & \frac{K}{2} \sum_{n=1}^{N-1} \mathbf{r}_n^2 - \sum_{k=1}^j Q_k \mathbf{E} \mathbf{r}_k - \sum_{k=j+1}^i (Q_k \mathbf{E} + f) \mathbf{r}_k \\ & - \sum_{k=i+1}^{N-1} Q_k \mathbf{E} \mathbf{r}_k - Q_{tot} \mathbf{E} \mathbf{R}_0 \end{aligned} \quad (12)$$

In Eq. (12) Q_{tot} denotes the total charge, $Q_{tot} = Q_0$. In the following we restrict first our considerations to neutral PAs for which the total charge Q_{tot} vanishes; we implement the extension to PAs with a non-vanishing net charge afterwards. For the partition function $Z = \int d\mathbf{r}_1 \dots d\mathbf{r}_{N-1} \exp(-U/T)$ we find readily that

$$\begin{aligned} Z = & \left(\sqrt{\frac{2\pi}{3}} b \right)^{3N-3} \prod_{n=1}^j \exp\left(-\frac{(Q_n \mathbf{E})^2 b^2}{6T^2} \right) \prod_{n=j+1}^i \exp\left(-\frac{(Q_n \mathbf{E} + f)^2 b^2}{6T^2} \right) \\ & \prod_{n=i+1}^{N-1} \exp\left(-\frac{(Q_n \mathbf{E})^2 b^2}{6T^2} \right) \end{aligned} \quad (13)$$

We proceed further by calculating the distance between a given pair of monomers i and j . In the following we take the Y -axis in the direction of the field \mathbf{E}

$$\mathbf{E} = (0, E, 0) \quad (14)$$

and set further $\mathbf{f} = (0, f, 0)$. The thermally averaged mean-squared Y -component of the distance between the i th and j th monomer, $\mathbf{P}_{ij} = \mathbf{R}_i - \mathbf{R}_j$ with $i > j$ can be evaluated by differentiating Z twice with respect to f , i. e.

$$\overline{Y_{ij}^2} = T^2 \left(\frac{1}{Z} \frac{\partial^2 Z}{\partial f^2} \right) \Bigg|_{f=0} = T^2 \frac{\partial^2}{\partial f^2} \ln Z|_{f=0} + T^2 \left(\frac{\partial}{\partial f} \ln Z|_{f=0} \right)^2 \quad (15)$$

Inserting Eq. (13) into Eq. (15) we find:

$$\overline{Y_{ij}^2} = \frac{b^2(i-j)}{3} + \frac{b^4 E^2}{9 T^2} \left(\sum_{k=j+1}^i Q_k \right)^2 \quad (16)$$

i. e., $\overline{Y_{ij}^2}$ is the sum of the usual Gaussian term and a field induced stretching. Since for the Gaussian chain the different Euclidean coordinates decouple (cf. Eq. (12)) the bead coordinates perpendicular to the field are not affected by the stretching and one has $\overline{X_{ij}^2} = \overline{Z_{ij}^2} = b^2(i-j)/3$. Setting in Eq. (16) $i = N-1$ and $j = 0$ we find for the thermally averaged mean-squared Y -component of the end-to-end vector $\mathbf{P} = \mathbf{R}_{N-1} - \mathbf{R}_0$:

$$\overline{P_Y^2} = \frac{b^2(N-1)}{3} + \frac{b^4 E^2}{9 T^2} \left(\sum_{k=1}^{N-1} Q_k \right)^2 \quad (17)$$

Before considering different charge distributions we note first how to handle PAs whose total charge does not vanish. In this case the center of mass (CM) moves under the influence of the field. In section 5 we calculate for different charge distributions the CM's drift motion under friction. Here, however, we are interested in the (internal) polymer conformations, which we relate to the position \mathbf{R}_{CM} of the CM, $\mathbf{R}_{CM} = \mathbf{R}_0 + \sum_{k=1}^{N-1} (N-k)\mathbf{r}_k/N$. The potential energy, Eq. (12) with $\mathbf{f} = 0$, can be rewritten as:

$$U(\{\mathbf{r}_n\}) = -Q_{tot} \mathbf{E} \mathbf{R}_{CM} + \frac{K}{2} \sum_{n=1}^{N-1} \mathbf{r}_n^2 - \sum_{k=1}^{N-1} \tilde{Q}_k \mathbf{E} \mathbf{r}_k \quad (18)$$

In Eq. (18) \tilde{Q}_k is a transformed charge variable defined by

$$\tilde{Q}_k = Q_k - \frac{N-k}{N} Q_{tot} \quad (19)$$

As usual the first term in Eq. (18) represents the total external force acting on the CM whereas the second and the third term are internal energy terms, which depend only on the internal coordinates $\{\mathbf{r}_k\}$. The thermal average over the internal conformations of a PA with $Q_{tot} \neq 0$ may be computed following the lines for a neutral PA by changing from Q to \tilde{Q}_k ; this corresponds to a change in the individual charges from q_k to

$$\bar{q}_k = q_k - Q_{tot}/N \quad (20)$$

We now turn to the study of PAs with prescribed distributions of charges. As a first example let us consider the case where only the end-beads are charged, namely $q_0 = -q$, $q_{N-1} = q$ and $q_k = 0$ otherwise. From this we have as cumulative charge variables $Q_k = q$ for $k = 1, \dots, N-1$ and $Q_0 = Q_{tot} = 0$. From Eq. (17) we find for the end-to-end distance

$$\overline{P_Y^2} = \frac{b^2(N-1)}{3} + \frac{b^4 q^2 E^2 (N-1)^2}{9T^2} \quad (21)$$

i.e. $\overline{P_Y^2}$ is the sum of the usual Gaussian term and a field-induced stretching term proportional to N^2 . Using Eq. (16) we find for the mean-squared distance between monomer i and j :

$$\overline{Y_{ij}^2} = \frac{b^2}{3} k + \frac{b^4 q^2 E^2}{9T^2} k^2 \quad (22)$$

with $k = i - j$. Hence, in the special case when the external forces act only on the ends of the chain the deformation is uniform: it depends only on the relative distance k , but it does not depend on the location (say $(i + j)/2$) along the chain.

In general, however, this is not the case. We demonstrate this for a charge distribution which mimics the classical tug of war, the symmetric diblock polyampholyte (SDP), namely $q_k = -q$ for $0 \leq k < N/2$ and $q_k = q$ for $N/2 \leq k < N$ (N even). Hence

$$Q_k = \begin{cases} kq & \text{for } k < N/2 \\ (N-k)q & \text{for } k \geq N/2 \end{cases} \quad (23)$$

From Eq. (16) we find for the local deformation of the segment between the monomers $i-1$ and i

$$\overline{Y_{i-1}^2} - \frac{b^2}{3} = \begin{cases} \frac{b^4 q^2 E^2}{9T^2} i^2 & \text{for } i < N/2 \\ \frac{b^4 q^2 E^2}{9T^2} (N-i)^2 & \text{for } i \geq N/2 \end{cases} \quad (24)$$

Thus from the ends to the middle of the chain the deformation increases. This can be understood as follows: The bond connecting the beads $i-1$ and i subdivides the chain in two parts, one consisting of the beads $n = 0, \dots, i-1$ with total charge $-Q_i$, the other one consisting of the beads $n = i, \dots, N-1$ with total charge Q_i . The external field E acts on the net charges of these two parts, which are connected by a spring with spring constant $K = 3T/b^2$, so that the deformation is given by $Q_i E/K$ resulting in Eq. (24) where one has the maximal deformation $qEN/(2K)$ at the middle of the chain. Further, using Eqs. (17) and (23) we find for the end-to-end distance

$$\overline{P_Y^2} = \frac{b^2(N-1)}{3} + \frac{b^4 q^2 E^2 N^4}{144 T^2} \quad (25)$$

i. e., a field-induced stretching proportional to N^4 .

We turn now to PAs where the charges are randomly positioned along the chain. Then it is necessary to perform an average with respect of different realisations of the charge distribution (denoted by brackets, $\langle \dots \rangle$). The mean-squared distance between two monomers, Eq. (16), takes then the form

$$\overline{\langle Y_{ij}^2 \rangle} = \frac{b^2(i-j)}{3} + \frac{b^4 E^2}{9 T^2} \sum_{k,l=j+1}^i \langle \tilde{Q}_k \tilde{Q}_l \rangle \quad (26)$$

for $i > j$.

We consider now random PAs with an uncorrelated distribution of charges, i. e. for which Eq. (9) holds. Since a given chain is not necessarily neutral one has to transform the charge distribution according to Eq. (20), from which we find

$$\langle \tilde{q}_k \tilde{q}_l \rangle = \left\langle \left(q_k - \sum_{i=0}^{N-1} q_i / N \right) \left(q_l - \sum_{j=0}^{N-1} q_j / N \right) \right\rangle = q^2 \delta_{kl} - q^2 / N \quad (27)$$

In ref.³⁶⁾ we have also investigated PAs whose charges are placed randomly along the chain, under the constraint of global neutrality $Q_{tot} \equiv 0$. Then the charge correlations are given by Eq. (7) with $Q_{tot} = 0$, i. e. these correlations are for large N approximately the same as the correlations $\langle \tilde{q}_k \tilde{q}_l \rangle$ of Eq. (27). This means that the following considerations are also valid for neutral PAs.

To evaluate $\langle P_Y^2 \rangle$ we need the correlations of the cumulative charge variables \tilde{Q}_k . From Eq. (27) we find for $k \geq l$:

$$\langle \tilde{Q}_k \tilde{Q}_l \rangle = \sum_{i=k}^{N-1} \sum_{j=l}^{N-1} \langle \tilde{q}_i \tilde{q}_j \rangle = q^2 \frac{(N-k)l}{N} \quad (28)$$

Inserting Eq. (28) into Eq. (26) we find for the distance between two monomers

$$\overline{\langle Y_{ij}^2 \rangle} = \frac{b^2 k}{3} + \frac{q^2 E^2 b^4}{36 T^2} \left[\frac{4k^2}{N} s (N-1-s) + \frac{2}{3} (k-k^3) + 2k^2 \right] \quad (29)$$

with $k = i - j$ and $s = (i + j)/2$. Especially for a subchain of length k centered around the middle of the PA (i. e. $s = N/2$) we find the following stretching term for $k \gg 1$:

$$\overline{\langle Y_{ij}^2 \rangle} - \frac{b^2 k}{3} \cong \frac{b^4 q^2 E^2}{36 T^2} \left[Nk^2 - \frac{2}{3} k^3 \right] \cong \begin{cases} \frac{q^2 E^2 b^4}{36 T^2} Nk^2 & \text{for } k \ll N \\ \frac{q^2 E^2 b^4}{108 T^2} N^3 & \text{for } k = N \end{cases} \quad (30)$$

The case $k \ll N$ follows simply from the fact that the typical excess charges of both halves of the chain are of order $\pm q\sqrt{N}/2$ (cf. Eq. (28) with $k = l = N/2$). The case $k = N$ in Eq. (30) represents the mean-squared end-to-end distance, namely

$$\overline{\langle P_Y^2 \rangle} = \frac{b^2 N}{3} + \frac{q^2 E^2 b^4 N^3}{108 T^2} \quad (31)$$

a result which we have first derived in refs.^{35,36} in the framework of the Rouse model (cf. also section 5.1). Another interesting special case is the situation at the chain's ends: Thus we find from Eq. (29) for $j = 0$ and $1 \ll i = k \ll N$ (i.e. $s = i/2$) for the deformation term $(q^2 E^2 b^4 / 27 T^2) k^3$, i.e. a k^3 -dependence (Note that here only the local charge distribution matters, so that N does not enter). By setting $k = 1$ we obtain the local deformation of the chain:

$$\overline{\langle Y_{s+1/2, s-1/2}^2 \rangle} - \frac{b^2}{3} \cong \frac{q^2 E^2 b^4}{36 T^2} \left[2 + \frac{4}{N} s(N-s) \right] \quad (32)$$

Hence for random PAs the mean-squared local deformation increases from the end to the middle of the chain. Let us finally calculate the mean-squared radius of gyration. Using Eq. (29) we find for $N \gg 1$:

$$\overline{\langle R_g^2 \rangle} = \frac{1}{2N^2} \int_0^N dn \int_0^N dm \overline{\langle P_{ij}^2 \rangle} \cong \frac{b^2 N}{6} + \frac{q^2 E^2 b^4}{810 T^2} N^3 \quad (33)$$

i.e., we find up to numerical constants the same scaling as for the mean-squared end-to-end distance, Eq. (31).

Sommer and Blumen⁴⁸ considered also generalized Gaussian structures such as membranes, gels and polymer networks with randomly charged monomers in the weak coupling limit. As long as the structure forms an isotropic and locally homogeneous fractal the radius of gyration (no interaction between the charges) scales in an external field as

$$\overline{\langle R_g^2 \rangle} \approx b^2 N^{(2-d_s)/d_s} + \frac{q^2 E^2 b^4}{T^2} N^{(4-d_s)/d_s} \quad (34)$$

Here d_s denotes the spectral dimension of the network⁴⁹. In the case of regular lattices d_s equals the Euclidean dimension d of the structure. Especially for a linear PA one has $d = 1$ and thus one recovers Eq. (33). Note that in the absence of an external field the structure collapses for $d_s \geq 2$, the marginal dimension being $d_s = 2$. The collapsed structure ($d_s > 2$), however, will unfold again under the influence of an external field E , as long as $d_s < 4$.

Due to its linearity the Gaussian chain model is only reasonable as long as the stretching is sufficiently small. A global criterion for the one-dimensional chain follows from the total deformation, by the requirement that the PA's mean-squared end-to-end distance in field direction, $\overline{\langle P_Y^2 \rangle}$, has to be much smaller than the end-to-end distance of a rodlike configuration, i.e. $\overline{\langle P_Y^2 \rangle} \ll b^2 N^2$. In the case of a random PA (cf.

Eq. (31)) this means that the external field E has to be restricted to the following range:

$$E \ll 10T/(qb\sqrt{N}) \quad (35)$$

A refined criterion follows from a local consideration: the maximal local deformation should be much smaller than b . From Eq. (32) we find for a random PA that E has to be much smaller than $6T/(qb\sqrt{N})$. Hence in the case of a random PA both criteria give an upper bound for E of the same order. Note that in the case of generalized Gaussian structures the range of allowed E -values may be much larger⁴⁸⁾. Requiring that the stretching term in Eq. (34) is much smaller than the size L of the unfolded structure, $L^2 \approx b^2 N^{2/d_s}$, one finds $E \ll (T/qb)N^{(d_s-2)/2d_s}$. Thus for $d_s > 2$ the external field may be quite strong without contradicting the Gaussian assumption.

3.2. Freely-jointed chain

For larger external fields the finite extensibility of the chain comes into play; this aspect can be accounted for by modeling the PA as a freely-jointed chain. We have considered this model in ref.³⁷⁾ and we report here some of our main results. As in section 3.1 we view the PA as consisting of N charged beads, connected into a chain by $N - 1$ links (bonds). Distinct from the Gaussian case these bonds have now a fixed length b . The PA is freely jointed⁵⁰⁾, i.e. each bond is able to point in any direction, independently of the other bonds. The potential energy has the form

$$U(\{\mathbf{r}_n\}) = -Q_{tot} \mathbf{E} \mathbf{R}_{CM} - \sum_{k=1}^{N-1} (\tilde{Q}_k \mathbf{E} + \mathbf{f}) \mathbf{r}_k \quad (36)$$

where the quantities \mathbf{r}_k , \tilde{Q}_k etc. have the same meaning as in section 3.1. For simplicity in Eq. (36) we restricted ourselves to the case in which the test force \mathbf{f} acts on the chain's ends only. As before this allows to determine readily the end-to-end distance. By integrating freely over the directions Ω_k of the \mathbf{r}_k -vectors we find for the partition function

$$Z = \int d\Omega_1 \dots d\Omega_{N-1} \exp(-U/T) = (4\pi)^{N-1} \prod_{k=1}^{N-1} \frac{\sinh((Q_k E + f)b/T)}{(Q_k E + f)b/T} \quad (37)$$

where we let \mathbf{E} and \mathbf{f} point in the Y -direction (cf. Eq. (14)).

Note that the partition function in Eq. (37) is *identical* to the partition function of $N - 1$ independent dipoles (with charges \tilde{Q}_k and $-\tilde{Q}_k$ at a distance b) in an external electrical field \mathbf{E} or, equivalently, to that of $N - 1$ magnetic dipoles in an external magnetic field; the later is a well-known problem in classical paramagnetism⁵¹⁾. This similarity follows from the fact that each bond (say the bond between $k - 1$ and k) subdivides the chain in two parts, one consisting of the beads $n = 0, \dots, k - 1$ with total charge $-\tilde{Q}_k$, the other one consisting of the beads $n = k, \dots, N - 1$ with total charge \tilde{Q}_k . The external field \mathbf{E} acts on the net charges of this two parts, which are connected by a bond of fixed length b , hence displaying the effective dipole $b\tilde{Q}_k$.

Following the lines of section 3.1 we find the mean-squared end-to-end distance in field direction by differentiating the partition function, Eq. (37), with respect to f . This results in

$$\overline{P_Y^2} = b^2(N-1) + b^2 \sum_{k=1}^{N-1} \sum_{l \neq k} L(\tilde{Q}_k Eb/T) L(\tilde{Q}_l Eb/T) - 2b^2 \sum_{k=1}^{N-1} \frac{L(\tilde{Q}_k Eb/T)}{\tilde{Q}_k Eb/T} \quad (38)$$

In Eq. (38) $L(x) = \coth x - 1/x$ is the Langevin function⁵¹⁾, which shows the following approximate behavior:

$$L(x) \cong \begin{cases} 1 & \text{for } 1 \ll x \\ x/3 - x^3/45 & \text{for } -1 \ll x \ll 1 \\ -1 & \text{for } x \ll -1 \end{cases} \quad (39)$$

Let us illustrate this again with the chain whose end-beads are charged, i.e. $q_0 = -q, q_{n-1} = q$ and $q_k = 0$ otherwise. Hence $Q_k = q$ for $k = 1, \dots, N-1$, and one finds for $N \gg 1$ from Eqs. (38) and (39) for the deformation

$$\overline{P_Y^2} \cong \frac{b^2 N}{3} + b^2 N^2 L^2(qEb/T) \cong \begin{cases} \frac{b^2 N}{3} + \left(\frac{qEb^2 N}{3T} \right)^2 & \text{for } E \ll T/(qb) \\ b^2 N^2 & \text{for } E \gg T/(qb) \end{cases} \quad (40)$$

For small fields we reproduce the Gaussian result, Eq. (21), whereas in the case of large external fields the PA becomes fully stretched. The crossover from the regime of linear response to the fully stretched case is described by the Langevin function. This is a well-known result for the extension of a freely-jointed chain when forces act on its end-beads only (see, for instance, Eq. (65) in chapter VIII of ref.⁵⁰⁾).

Another fixed charge distribution which we investigated is the alternating one. In the high field limit an alternating PA of an odd polymerisation degree N collapses, whereas for N even the PA becomes highly stretched. We refer the interested reader to ref.³⁷⁾.

Let us now turn to random PAs. Then the mean-squared end-to-end distance $\overline{P_Y^2}$ has to be averaged with respect to the realisations of $\{q_k\}$. Hence we have either to evaluate $\langle \ln Z \rangle$ (cf. Eq. (15)) or forms such as $\langle L(c_1 \tilde{Q}_k) L(c_2 \tilde{Q}_l) \rangle$ (cf. Eq. (38)), both of which are difficult tasks. Thus we use the approximate expressions for the Langevin function, Eq. (39), to calculate $\langle \overline{P_Y^2} \rangle$ from Eq. (38) in the limits of weak and of strong fields. Following this strategy we find for weak fields:

$$\langle \overline{P_Y^2} \rangle \cong \frac{b^2(N-1)}{3} + \frac{b^4 E^2}{9T^2} \sum_{k=1}^{N-1} \sum_{l \neq k} \langle \tilde{Q}_k \tilde{Q}_l \rangle + \frac{2E^2 b^4}{45T^2} \sum_{k=1}^{N-1} \langle \tilde{Q}_k^2 \rangle \quad (41)$$

Since usually the third term of Eq. (41) is of the order $1/N$ smaller than the second one we recover for small fields the behavior of the Gaussian model, Eq. (17). For strong fields we find from Eqs. (38) and (39):

$$\langle \overline{P_Y^2} \rangle = \frac{b^2}{3} \langle n_0 \rangle + b^2 \langle (n_+ - n_-)^2 \rangle \quad (42)$$

Here n_+ , n_- and n_0 denote the number of \tilde{Q}_k with $\tilde{Q}_k > 0$, $\tilde{Q}_k < 0$ and $\tilde{Q}_k = 0$, respectively.

Inserting the correlations of the cumulative charge variable, Eq. (28), into Eqs. (41) and (42), the mean-squared deformation for a PA with an uncorrelated charge distribution follows. In the limit of small fields, $E \ll T/(bq\sqrt{N})$ we recover for $N \gg 1$ the result of the Gaussian chain, Eq. (31). For large external perturbations we have to know the probability distributions of n_+ , n_- and n_0 (cf. Eq. (42)). For large N these distributions can be deduced from results of random walk theory. Note that the set $\{\tilde{Q}_k\}$ can be interpreted as being the path of a Brownian particle starting at $\tilde{Q}_0 = 0$ and arriving after N elementary steps \tilde{q}_k ($k = 0, \dots, N-1$) at $\tilde{Q}_{N-1} = 0$. For such Brownian bridges it is a well-known result that the sojourn times on the positive side, i.e. n_+ , or on the negative side, i.e. n_- , are equally distributed (cf. the equidistribution theorem of section III.9 of ref.⁵²). Ignoring $\langle n_0 \rangle$ which is of order \sqrt{N} , the probability p_+ (p_-) of having precisely n_+ (n_-) steps on the positive (negative) side obeys very well $p_+ = p_- = N^{-1}$. Hence from Eq. (42) the end-to-end distance in the case of large external fields, $E \gg T/(bq)$ follows:

$$\overline{\langle P_{\tilde{y}}^2 \rangle} \cong \frac{b^2}{N} \sum_{k=0}^N (2k - N)^2 = \frac{b^2 N^2}{3} \quad (43)$$

Therefore the mean-squared end-to-end distance is a third of the squared length of a rodlike chain. This reflects the fact that typically some bonds are in the direction of the field (say n_+ ones) whereas n_- bonds are directed opposite to the field, resulting in a random, zigzag configuration.

3.3. Excluded volume chain

The models of PAs in the previous sections take no excluded volume effect into account; this limits their applicability to the θ -domain: In ref.³⁴ we discussed swollen PAs by using scaling arguments. Here we provide some additional results.

We have to modify an approach going back to Pincus⁵³ (cf. also ref.⁴³) which we briefly recall here. Pincus considered a single chain under traction where the forces F and $-F$ are applied to the ends. This can, for instance, be realized for a chain with charged end-beads, $q_0 = -q$, $q_{N-1} = q$ and $q_k = 0$ otherwise, so that $F = qE$. The elongation ΔL of the chain may be written as

$$\Delta L = L(F) - L = L\varphi\left(\frac{L}{\xi}\right) \quad (44)$$

with a dimensionless function φ . Here $L = L(0)$ denotes the end-to-end distance of the unperturbed chain $L = bN^\nu$ (with $\nu = 3/5$ in a good solvent and $\nu = 1/2$ in a θ -solvent), and $\xi = T/F$ with $F = |F|$. Now ξ is a characteristic length of the problem: For small F , $L/\xi \ll 1$, the response is linear in F , i.e. $\varphi(x) \propto x$, and thus $\Delta L \propto L^2 F/T$, i.e.,

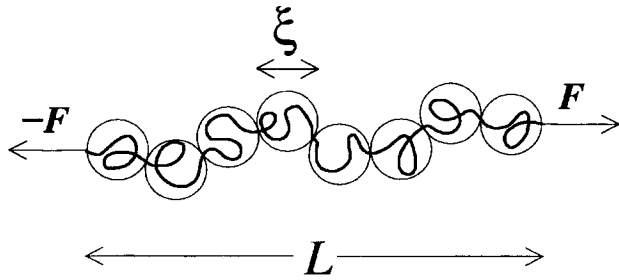
$$\Delta L \cong \frac{b^2 N^{2\nu} F}{T} \quad (45)$$

Thus in a good solvent the response for small external perturbations is non-linear in N . For large F , $L\xi \gg 1$, the chain breaks up into a string of independent blobs, each of size ξ (cf. Fig. 1). Inside the blob the external force induces only a small perturbation so that one has a swollen (ideal) subchain consisting of $g = (\xi/b)^{1/\nu}$ monomers. The elongation of the whole chain is then given by $\Delta L \equiv (N/g)\xi$, i.e.,

$$\Delta L \equiv Nb \left(\frac{bF}{T} \right)^{(1-\nu)/\nu} \equiv \begin{cases} Nb \frac{bF}{T} & \text{in a } \theta\text{-solvent} \\ Nb \left(\frac{bF}{T} \right)^{2/3} & \text{in a good solvent} \end{cases} \quad (46)$$

Note that in this regime the response of the excluded volume chain is linear in N but non-linear in the applied force.

Fig. 1. Free polymer under traction F . The chain breaks up into a string of Pincus blobs of equal sizes $\xi = T/F$



Let us now consider a PA with a given charge distribution $\{q_k\}$. Then, distinct from the original Pincus problem we encounter here in general a situation where the force is non-uniform (n -dependent) along the chain: Following the discussion in section 3.1 the force acting on the segment between the monomers n and $n+1$ is proportional to the (rescaled) cumulative charge variable \tilde{Q}_n and is given by $F_n = \tilde{Q}_n E$. Thus we need in the following a generalization of Eqs. (45) and (46) for non-uniform stretching. We follow here an argument given by Brochard-Wyart, who considered the non-uniform deformation of tethered chains in strong external flows⁵⁴. We denote by $\xi_n = T/F_n$ the (n -dependent) blob sizes, by $g_n = (\xi_n/b)^{1/\nu}$ the number of monomers of the blob to which n belongs and by l_n the position of the n th monomer in the direction of the field. In the case of small fields (i.e. $L\xi_n \ll 1$ for all n) we find from Eq. (45) for the local behavior at monomer n

$$dl_n \equiv \frac{b^2 F_n}{T} n^{2\nu-1} dn \quad (47)$$

On the other hand in the strong field regime the local behavior at n follows from Eq. (46):

$$dl_n \equiv \frac{\xi_n}{g_n} dn \quad (48)$$

Let us illustrate this scaling picture for a SDP, where the cumulative charge variable is given by Eq. (23). For small deformations, i.e. $E \ll T/(qbN^{1+\nu})$, one finds from Eq. (47) by integrating over n

$$\Delta L \cong \frac{b^2 q E}{T} N^{2\nu+1} \quad (49)$$

a result which is similar to the uniform deformation when one replaces F in Eq. (45) by an effective force qEN . Eq. (49) describes very small deformations where $\Delta L \ll bN^\nu$, i.e. one has a weakly perturbed swollen chain configuration; the case of large deformations follows from Eq. (48):

$$dl_n \cong \begin{cases} an^{(1-\nu)/\nu} dn & \text{for } n < N/2 \\ a(N-n)^{(1-\nu)/\nu} dn & \text{for } n \geq N/2 \end{cases} \quad (50)$$

where $a = (qET)^{(1-\nu)/\nu} b^{1/\nu}$. By integrating we have from Eq. (50) $l_n \cong an^{1/\nu}$ for $n < N/2$ and $l_n = 2l_{N/2} - l_{N-n}$ for $n \geq N/2$. Setting $n = N$ we find for the total deformation of the chain $\Delta L \cong aN^{1/\nu}$, a result which can also be revealed by inserting in Eq. (46) the effective force $F_{eff} \approx qEN$. Especially in the case $\nu = 1/2$ (θ -solvent) the total deformation for large external fields obeys $\Delta L \cong (b^2 q E/T) N^2$, a result which also holds in the limit of small fields, Eq. (49). Thus, in the absence of excluded volume effects, this argument predicts no crossover between different scaling regimes and one recovers (up to a numerical constant) the result of the exact calculations, Eq. (25).

The scaling picture for the highly deformed state contains much more information than the displacement of the monomers, l_n . It is also possible to derive the typical overall shape from the geometry of the Pincus blobs. For $n < N/2$ ($n \geq N/2$) we find $\xi_n \propto F_n^{-1} \propto n^{-1}$ ($\xi_n \propto (N-n)^{-1}$), i.e. we have a series of blobs whose sizes increase towards both ends as shown in Fig. 2. More precisely, making use of $l_n \propto n^{1/\nu}$ we find that to the left of Fig. 2 the blob sizes increase with decreasing l as $\xi_{n(l)} \propto n(l)^{-1} \propto l^{-\nu}$ as indicated in the figure; the exponent equals $-3/5$ for a swollen chain and $-1/2$ for an ideal chain. The same argument holds for the other end of the chain, i.e., the conformation is symmetric around the middle blob. This shape can be compared with the typical conformation of a tethered chain in a strong flow⁵⁴: There the

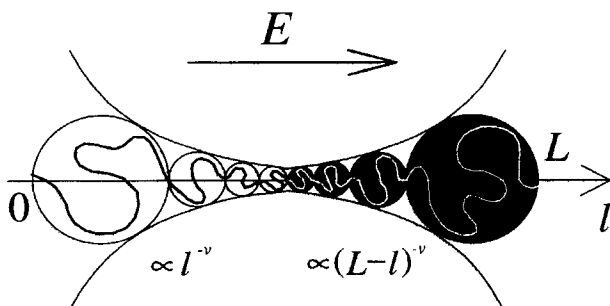


Fig. 2. Equilibrium conformation of a symmetric diblock polyampholyte (SDP) in an external electrical field (tug of war). The chain consists of a string of Pincus blobs of different sizes $\xi_{n(l)}$ and the global shape is trumpet-like at both ends

forces (blob sizes) decrease (increase) from the grafted site to the free end, so that the chain attains a trumpet-like shape. Thus a polymer exposed to a tug of the war shows a similar shape, having, however, two trumpet-like ends.

Note that one has a here rather pronounced stretching of the PA with $\Delta L \propto N^{1/\nu}$. Due to their finite extensibility real PAs will show a crossover from this regime to stretched configurations, in which the bonds are directed parallel to the external field. The onset of this effect occurs in the middle of the chain when $\xi_{N/2} \approx b$ so that there the Pincus-blob picture breaks down. This means that at a field strength of $E \approx T/(qbN)$ a regime with a completely stretched middle chain portion sets in. At both ends of the chain, however, one still has a Pincus behavior. A similar coexistence feature was discussed by Brochard-Wyart for polymer chains under strong flows and was called the “stem and flower”-regime⁵⁵. Here, in the classical tug of war situation, for sufficiently large E the PA’s conformation consists of two flowers connected by a stem.

Let us now discuss random PAs in terms of this scaling approach. In order to simplify the calculations and to get a clearer picture we use in the following a *preaveraged* charge distribution. From Eq. (28) we find for the mean-squared cumulative charge variable $\langle \tilde{Q}_n^2 \rangle \cong q^2 fn(1 - n/N)$. We use in the following

$$\tilde{Q}_n = \sqrt{\langle \tilde{Q}_n^2 \rangle} = q\sqrt{fn(1 - n/N)} \quad (51)$$

instead of \tilde{Q}_n . For small external fields we find from Eq. (47) by integration

$$\begin{aligned} l_n &\cong \frac{\sqrt{f}qEb^2}{T} N^{2\nu+1/2} \int_0^{n/N} dx x^{2\nu-1/2}(1-x)^{1/2} \\ &= \frac{\sqrt{f}qEb^2}{T} N^{2\nu+1/2} B\left(2\nu + \frac{1}{2}; \frac{3}{2}; \frac{n}{N}\right) \end{aligned} \quad (52)$$

with B being the incomplete beta function (cf. Eq. 58.3.1 of ref.⁵⁶). Setting $n = N$ the total deformation follows:

$$\Delta L \cong \frac{\sqrt{f}qEb^2}{T} N^{2\nu+1/2} \frac{\Gamma(2\nu + 1/2)\Gamma(3/2)}{\Gamma(2\nu + 2)} \approx \frac{\sqrt{f}qEb^2}{T} N^{2\nu+1/2} \quad (53)$$

(cf. 43.13.2 of ref.⁵⁶) for the evaluation of the integral). The crossover to large tensions (Pincus regime) is given when the sizes of the Pincus blobs become comparable to the radius of the unperturbed chain. Now, in the preaveraged picture the sizes of the Pincus blobs obey

$$\xi_n \cong \frac{T}{\sqrt{fn(1 - n/N)}qE} \quad (54)$$

i. e., in this picture we have a series of blobs whose sizes increase towards both ends (cf. Fig. 3). Thus using the smallest blob as reference, the crossover to the Pincus regime sets in at $\xi_{N/2} \approx bN^\nu$. This translates into the following condition for the Pincus regime:

$$E \gg E_1 = \frac{T}{\sqrt{fN}qbN^\nu} \quad (55)$$

For $E < E_1$ the deformation of the chain is given by Eqs. (52) and (53). For $E \gg E_1$ we have to insert Eq. (54) into Eq. (48) and to integrate from 0 to n ; this results in

$$l_n \cong \beta \int_0^{n/N} dx (x(1-x))^{(1-\nu)/(2\nu)} = \beta B\left(\frac{1+\nu}{2\nu}; \frac{1+\nu}{2\nu}; \frac{n}{N}\right) \quad (56)$$

with $\beta = b^{1/\nu} (\sqrt{f}qE/T)^{(1-\nu)/\nu} N^{(1+\nu)/(2\nu)}$. From Eq. (56) it follows that the deformation is symmetric with respect to the middle of the chain. The deformation around one of the chain's ends, say the end which contains the monomer $k = 1$ obeys $l_n \propto n^{(1+\nu)/(2\nu)}$ for $n \ll N$ (cf. Eq. (56)), a result which we also found analytically for the Gaussian chain ($\nu = 1/2$; cf. the discussion after Eq. (31)). Thus to the left of Fig. 3 the blob

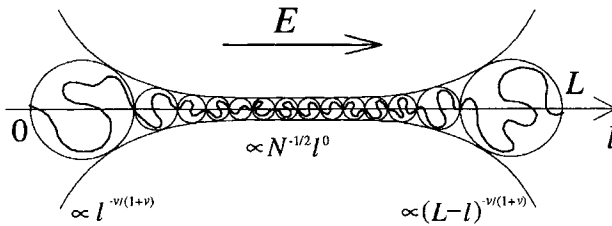


Fig. 3. Equilibrium conformation of a random PA in external fields. The PA's shape for the preaveraged charge distribution is shown (see text for details)

sizes increase with decreasing l as $\xi_{n(l)} \propto n(l)^{-1/2} \propto l^{-\nu/(1+\nu)}$, which we indicated in the figure; the exponent equals $-3/8$ for a swollen chain and $-1/3$ for an ideal chain. The middle of the chain shows another scaling behavior: From Eq. (56) one finds for a subchain of length m ($m \ll N$): $l_{N/2} - l_{N/2-m} \propto mN^{(1-\nu)/(2\nu)}$ (cf. Eq. (30) for the θ -case). This is due to the typical charge fluctuations of both halves of the chain. Thus the chain's central part consists of equally sized Debye blobs with $\xi_{n(l)} \propto N^{-1/2} l^0$ (cf. Eq. (54) and Fig. 3).

To obtain the end-to-end distance we set in Eq. (56) $n = N$ and find

$$\Delta L \cong \beta B\left(\frac{1+\nu}{2\nu}; \frac{1+\nu}{2\nu}; 1\right) = \beta \frac{\Gamma^2((1+\nu)/(2\nu))}{\Gamma((1+\nu)/\nu)} \approx \beta \quad (57)$$

i. e., explicitly

$$\Delta L \approx \begin{cases} bN \frac{\sqrt{fN}qEb}{T} & \text{in a } \theta\text{-solvent} \\ bN \left(\frac{\sqrt{fN}qEb}{T}\right)^{2/3} & \text{in a good solvent} \end{cases} \quad (58)$$

For the θ -case we hence recover with Eq. (58) (up to a numerical constant) the result for Gaussian chains, Eq. (31). The excluded volume chain shows a similar non-linear response as in the case of a uniform deformation, cf. Eq. (46); one has simply to replace F by an effective force of the order $F_{\text{eff}} \approx \sqrt{fN}qE$. This simplified picture of equally sized Pincus blobs is called *monoblock approximation*⁵⁷⁾ and will be used in section 5.2.

Due to Eq. (58) we have here a rather pronounced stretching of the chain with $\Delta L \propto N^{(1+\nu)/(2\nu)}$. Thus at a sufficiently large external field $E = E_2$ we have a crossover from the Pincus regime to the stem and flower-regime with completely stretched portions of the chain (stems). In the preaveraged picture the onset of this effect is predicted to occur in the middle of the chain when $\xi_{N/2} \approx b$. This means that the field strength E_2 with

$$E_2 = \frac{T}{\sqrt{fN}qb} \quad (59)$$

marks the border between the Pincus regime, Eq. (58) ($E < E_2$) and the regime of stretched chain configurations ($E \gg E_2$). As shown in section 3.2 for the freely-jointed chain, in this regime one has $L^2 = b^2N^2/3$ for the mean-squared end-to-end distance of the stretched chain configuration (cf. Eq. (43)). Note that for large N the Pincus regime occurs for a rather broad interval of E -values, namely $E_1 < E < E_2 \cong N^{\nu}E_1$.

The scaling approach discussed in this section shows how a given charge distribution translates into the PA's overall shape (i.e., a sequence of Pincus blobs as depicted, for instance, in Fig. 2) when the chain is exposed to an external field E . The other way around one may ask the following question: Suppose one aims to have a set of Pincus blobs whose sizes obey

$$\xi_{n(l)} = f(l) \quad (60)$$

with $0 < l < L$ (cf. Fig. 4); how does one have to choose the sequence of charges q_n such that Eq. (60) is fulfilled? To be more precise: Suppose that Eq. (60) is given together with E , T , b and the solvent quality, i.e., ν . As we will see the function f has to fulfil several conditions: (I) $\lim_{l \rightarrow 0} f(l) = \lim_{l \rightarrow L} f(l) = \infty$, (II) f has to be continuous and piecewise differentiable, (III) $f^{(1-\nu)/\nu}$ has to be integrable on the interval $0 \leq l \leq L$, and (IV) evidently $f(l) \geq 0$ for $0 < l < L$, where the equality sign holds only at isolated values. Then the length of the PA, N , and its charge distribution can be evaluated as follows. One has to start from the relation $F_n = T/\xi_n = Tf(l(n))$ together with $F_n = \tilde{Q}_n E = E \int_0^n dk \tilde{q}_k$ (from which automatically condition (I) follows, since $\tilde{Q}_0 = \tilde{Q}_N = 0$). We find immediately

$$\tilde{q}_n = \frac{1}{E} \frac{\partial F_n}{\partial n} = \frac{T}{E} \frac{f'(l(n))l'(n)}{f^2(l(n))} \quad (61)$$

(here we need condition (II)). Thus we have to determine now the function $l(n)$. From Eq. (48) we find

$$\frac{dn(l)}{dl} = \frac{1}{b^{1/\nu}} \xi_{n(l)}^{(1-\nu)/\nu} = \frac{1}{b^{1/\nu}} (f(l))^{(1-\nu)/\nu} \tag{62}$$

from which the inverse function of $l(n)$ follows by integration (with $n(0) = 0$)

$$n(l) = \frac{1}{b^{1/\nu}} \int_0^l d\lambda (f(\lambda))^{(1-\nu)/\nu} \tag{63}$$

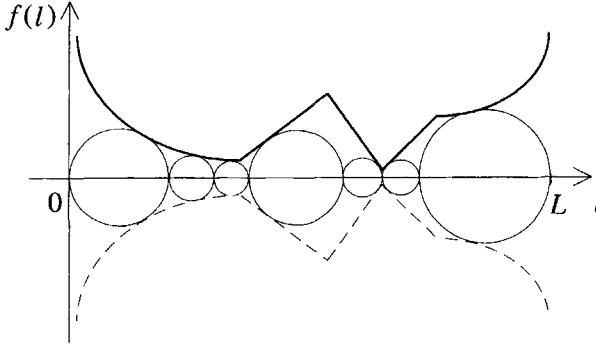


Fig. 4. Polyampholyte in an external field consisting of a string of Pincus blobs with given sizes $\xi_{n(l)} = f(l)$. From this the sequence of charges which induce this shape can be determined (see text)

Due to the condition (III) the integral exists for the function f considered and the implicit relation for Eq. (63) can be inverted (due to condition (IV)), giving $l(n)$. Furthermore from Eq. (63) $N = n(L)$ follows. Using Eq. (62) together with $n'(l(n)) = 1/l'(n)$, Eq. (61) can be reformulated as follows:

$$\hat{q}_n = \frac{b^{1/\nu} T}{E} \frac{f'(l(n))}{(f(l(n)))^{(1+\nu)/\nu}} \tag{64}$$

Thus we have found a receipt how to choose the charge distribution in order to obtain a sequence of Pincus blobs with preassigned sizes: First calculate Eq. (63) to get $n(l)$ and thereby $N = n(L)$ and $l(n)$; then q_n ($0 \leq n \leq N$) follows from Eq. (64). Note that for an arbitrary constant c $q_n = \hat{q}_n + c$ is also a solution of the problem (leading to a PA with a total charge $Q_{tot} = cN$; cf. also the discussion in section 3.1).

To give an example consider a double trumpet-like shape with

$$f(l) = \begin{cases} cl^\gamma & \text{for } 0 < l \leq L/2 \\ c(L-l)^\gamma & \text{for } L/2 < l < L \end{cases} \tag{65}$$

The conditions for f restrict the parameters to $c > 0$ and $-\nu/(1-\nu) < \gamma < 0$. From Eq. (63) we find for $0 < l \leq L/2$ $n(l) = \mu l^{1+\gamma\kappa}$ with $\kappa = (1-\nu)/\nu$ and $\mu = (1+\gamma\kappa)^{-1} c^\nu/b^{1/\nu}$; for $L/2 < l < L$ we have $n(l) = 2n(L/2) - n(L-l)$ and N is given by $N = 2n(L/2)$. Inversion of $n(l)$ results in

$$l(n) = \begin{cases} (n/\mu)^{1/(1+\gamma\kappa)} & \text{for } 0 \leq n \leq N/2 \\ L - ((N-n)/\mu)^{1/(1+\gamma\kappa)} & \text{for } N/2 < n \leq N \end{cases} \tag{66}$$

Finally, we find from Eq. (64) for the distribution of charges:

$$\bar{q}_n = \begin{cases} \gamma \frac{(b/c)^{1/\nu}}{E/T} (n/\mu)^{-\frac{\nu+\gamma}{\nu(1+\gamma\kappa)}} & \text{for } 0 \leq n \leq N/2 \\ -\gamma \frac{(b/c)^{1/\nu}}{E/T} ((N-n)/\mu)^{-\frac{\nu+\gamma}{\nu(1+\gamma\kappa)}} & \text{for } N/2 < n \leq N \end{cases} \quad (67)$$

i. e., an algebraic n -dependence of \bar{q}_n for each half of the polymer and a change of the sign in the middle of the chain. The special case $\gamma = -\nu$ corresponds to the SDP discussed above.

4. Conformational properties of PAs in external fields (strong coupling)

In this section we study the behavior of PAs in the case of strong interactions between the charges (strong coupling case), i. e., when Eq. (5) is fulfilled. In the absence of an external field, as discussed in subsection 2.1, neutral PAs form globules of densely packed Debye blobs. As we have shown in ref.³⁴⁾ up to a critical field E_c the PA's response to external fields E is controlled mainly by the surface tension; an instability is predicted for $E = E_c$: For $E > E_c$ the PA is highly extended. We report in subsection 4.1 this surface controlled scenario and discuss the PA's conformational properties of the extended state in subsection 4.2.

4.1. Drop analogy

From the discussion of the collapsed state in subsection 2.1 we inferred for the PA globule the fixed volume condition, Eq. (4). Thus we are concerned with incompressible PAs. Their shapes, however, are controlled by other mechanisms, such as the competition between the surface tension and the external perturbations. The free energy of the surface is of the form

$$F_S = \gamma S \quad (68)$$

where S denotes the PA's surface and γ the surface tension. Following Dobrynin and Rubinstein²¹⁾ γ can be estimated by noting that each thermal blob at the surface has (because of missing neighboring blobs) an additional energy of order T . Since the radius of these blobs is of the order of the screening length r_D one finds for the surface tension

$$\gamma \approx T/r_D^2 \quad (69)$$

In the absence of an external electrical field the PA minimizes its surface energy, Eq. (68) by taking a spherical shape — a situation which is reminiscent of a fluid drop.

Here we consider the case of a neutral PA in an external electrical field. Related situations obtain when one applies external electrical fields to dielectric or conduct-

ing drops (see ref.⁵⁸⁾ and references therein). Thus a conducting, fluid drop of conductivity σ_1 suspended in a fluid of conductivity σ_2 , where $\sigma_2 < \sigma_1$, shows the following response to the external perturbations: Under small electrical fields the drop undergoes only a smooth deformation, under larger fields it takes a dumbbell-like shape. Under a further increase of the field the drop lengthens rapidly; it becomes divided into two blobs connected by a thin thread, before the final breakup occurs. For $\sigma_1 \gg \sigma_2$ the response to the external field is different: both ends of the drop become pointed and start to eject charged droplets. The ratio of conductivities dividing these two types of mechanisms lies around $\sigma_1/\sigma_2 \approx 30$.

The situation of a neutral PA in an external field is related to the above. If one has an annealed charge distribution, i. e., if the charges can move freely along the chain and follow the field, a response similar to tip-formation mechanism may occur. Due to connectivity it is, however, not possible for a PA to eject droplets, but it can lower its energy by extruding charges along fingers at the two ends. A similar situation may also occur when the annealed PA carries a non-vanishing charge; the polymer can lower its energy by forming charged, protruding fingers²²⁾.

Here we are, however, interested in the usual case of quenched charge distributions. Due to the connectivity of the chain, the positive and the negative charges cannot be arbitrarily separated. The situation can be envisaged as follows: Consider that a neutral PA chain is divided into two halves; on the average they have excess charges of opposite sign, which are typically of the order $q\sqrt{fN}$. When a sufficiently large external field is applied we expect that these halves will rearrange themselves so as to minimize the free energy. A way to achieve this is through a deformation of the incompressible PA volume, similarly to the previously mentioned dumbbell. Note that the fixed volume (incompressibility) condition is not affected by the presence of a not-too-strong external field: The major part of the monomers is still organized in blobs according to the Debye-Hückel prescription.

Here we use a simple liquid-like (fixed volume, see Eq. (4)) model for the PAs; then only the PAs' shapes may vary. Furthermore we have to restrict the whole spectrum of possible shapes to a reasonable small subclass. Since we expect that under external fields the PAs will follow similar deformation scenarios as conducting drops (especially the formation of a neck) we start from a dumbbell-like structure as shown in Fig. 5a. It consists of two spheres of equal size which overlap each other. We let one of them carry a total charge of $q\sqrt{fN}$, so that the other one carries $-q\sqrt{fN}$. The dumbbell-structure takes implicitly into account that the charges are

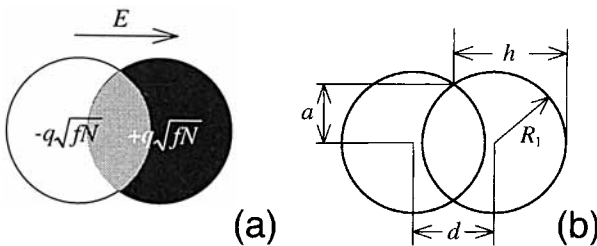


Fig. 5. Neck formation of a PA globule in an external electrical field. Here a simplified geometrical shape is depicted: (a) charge distribution and (b) geometrical parameters. The figures display cross-sections of the cylindrically-symmetric dumbbell

connected via the PA backbone. Our picture leads to an effective dipole, and to a one-parameter family of shapes which depend — for a fixed total volume V — only on the distance d between the centers of the spheres (see Fig. 5b). Due to its simple geometrical form this model has the advantage of being analytically tractable. We speculate that this class of shapes represents a good approximation to the equilibrium shapes of real PAs under moderately strong external fields; this holds good up to a critical electric field E_c at which the whole structure breaks down, see below.

Let us calculate now the potential (free) energy F_{ext} of the effective dipole and the surface free energy F_S , Eq. (68), as a function of the distance d between the centers. F_{ext} has for an external field E the form:

$$F_{ext}(d) = -q\sqrt{fN} E d \quad (70)$$

where we set, for simplicity, the dielectric constant ϵ of the medium to be unity. To evaluate F_S we need to know the surface of the dumbbell as a function of d , i. e. $S = S(d)$. The surface is simply given by the surface of the two intersecting spherical portions. We find by simple integration

$$S = 4\pi h R_1 = 4\pi h(h - d/2) \quad (71)$$

with R_1 being the radius of the spheres, and $h = R_1 + d/2$ the height of the portions (see Fig. 5b). Furthermore d has to be confined to the interval $0 \leq d \leq 2^{2/3}R$ the lower limit corresponding to one (neutral) sphere, with radius $R = (3V/(4\pi))^{1/3}$, the upper limit to two smaller spheres of opposite charge, attached at one point. Now h has to be chosen such that the fixed volume condition is fulfilled. Hence, again through integration, we have

$$\frac{2\pi}{3} h^2(3R_1 - h) = V \quad (72)$$

with V being given by Eq. (4). From Eq. (72) $h = h(d)$ and then $S = S(d)$ follows (see ref.³⁴) for explicit formulas). Minimizing $F' = F_{ext} + F_S$ with respect to d we find further $d = d(E)$ and thus the increase of the PA-length L in field direction:

$$L(E) = 2h(d(E)) \cong R \left(\frac{5}{3} + \frac{5}{16} (1 + \alpha E)^{1/2} + \frac{1}{16} \alpha E + \frac{1}{48} (1 + \alpha E)^{3/2} \right) \quad (73)$$

with $\alpha = 4\sqrt{fN}q/(\pi\gamma R)$. For $E\alpha \ll 1$ the PA's extension $\Delta L = L(E) - L(0)$ is linear in the external field:

$$\Delta L \cong \frac{\sqrt{fN} q E}{\pi\gamma} \quad (74)$$

The dumbbell shape is, however, stable only for external fields E below a critical value E_c . At $E = E_c$ the neck has become so narrow that the PA can lengthen rapidly by forming a bridge between the two blobs. The critical value E_c can be estimated as follows: The radius a of the neck is given by $a^2 = h(2R_1 - h) = h(h - d)$ (cf.

Fig. 5b). The dumbbell becomes unstable when the external electrical field is so large that there exists an infinitesimal deformation where the increase of the surface energy equals the decrease in the electrical potential. The ‘weak point’ of the dumbbell is located at its neck. When there a cylindrical bridge of radius a and (infinitesimal) height dL is formed, the change in surface energy is given by $dF_S = 2\pi\gamma a dL$, whereas we find for the electrical potential $dF_{ext} = -\sqrt{fN} qEdL$. Thus the dumbbell becomes unstable at $E = E_c$ with E_c given by

$$E_c \cong 4.06a^{-1} \cong 3.19 \frac{\gamma R}{\sqrt{fN} q} \quad (75)$$

(see ref.³⁴⁾ for details). With this result we obtain for $E = E_c$ the geometrical parameters which characterize the dumbbell: they are $d \cong 1.25 R$, $a \cong 0.5 R$, $h \cong 1.43 R$ and $R_1 \cong 0.81 R$.

At $E \cong E_c$ the surface tension cannot counterbalance the electrical force anymore and the PA lengthens rapidly. The PA takes an extended configuration which we discuss in the next section.

4.2. The extended state

In the following we use scaling arguments similar to section 3.3 to analyse the extended state of the PA in strong fields. First, let us mentally switch off the electrostatic interaction between the charges; as we will see, the interaction can be incorporated easily *a posteriori*. Without the coupling between the charges we have (in the preaveraged picture) the situation depicted in Fig. 3. Here the sizes of the Pincus blobs are given by Eq. (54), the positions of the monomers by Eq. (56) and the total elongation obeys Eq. (58).

Let us now consider the role of the electrostatic interactions between the charges. Note that the critical electrical field E_c , cf. Eq. (75), which is necessary to induce a breakup of the globule, is strong enough to fulfil condition (55), since $E_c/E_1 \approx (R/r_D)(bN^v/r_D)$ is obviously much larger than unity. The blob picture given above remains unchanged for Pincus blobs with $\xi_n < r_D$. For such blobs the electrostatic energy, Eq. (2), is smaller than T so that the interaction between the charged monomers is only a small perturbation. For $\xi_n > r_D$ each Debye blob inside the Pincus blob contributes an electrostatic free energy of the order T , so that one has roughly $Tg_n/g_D = T(\xi_n/r_D)^{1/v}$ for the electrostatic energy of the whole Pincus blob. Thus for these blobs the Debye-Hückel mechanism discussed in section 2.1 comes into play and one has instead of such a Pincus blob a condensed set (condensate) of closely packed Debye blobs.

In the preaveraged picture where the blob sizes are given by Eq. (54) the larger Pincus blobs are located at the ends of the chain. These are candidates to become condensates of Debye blobs. Consider the half chain containing the bead with $n = 0$. Here any given monomer n may belong to a condensate as long as $\xi_n > r_D$, i. e. as long as $n < n_1$ with $n_1(E) = (T/(\sqrt{f}qEr_D))^2$. This means, however, that immediately after the breakup of the PA for $E = E_c$ only a very small amount of the material

is still found in such condensates, since $2n_1(E_c)/N \approx r_D^2/R^2 \ll 1$ holds. Thus Eq. (58) is also in the strong coupling case a good approximation for L .

For a given realization $\{q_n\}$ of the charge distribution the extended conformation may deviate from this ‘typical’ picture. Instead of the preaveraged Eq. (54), the size of the Pincus blob around the n th monomer is given by $\xi_n \cong T/(Q_n E)$. Thus there may occur condensates of blobs along the chain at the positions (say n) for which $\xi_n > r_D$ holds. Especially, if the cumulative charge variable Q_n changes its sign at the monomer position n_0 then one has around n_0 a condensate. A further effect which occurs at such changes of sign is that the external force acting on the segments before and after n_0 changes its direction so that the PA may become folded. In Fig. 6 we sketch such a conformation.

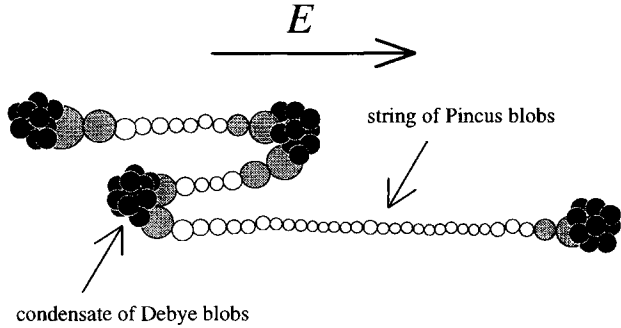


Fig. 6. Configuration of a randomly charged PA for large field strength $E > E_c$. Schematically depicted is a typical conformation above the instability range. The chain consists of strongly stretched portions (strings of Pincus blobs) and of condensates of Debye blobs; the latter are to be found at the ends and at turning points of the zig-zag conformation (see text for details)

In subsection 3.3 we have shown that the Pincus picture breaks down for field strengths $E \gg E_2$ (cf. Eq. (59)) where one has stretched chain configurations (stem and flower-regime). In our problem the Pincus regime, Eq. (58), occurs only when $E_c < E_2$, i. e. when $b > N^\delta f l_B$ with $\delta = 1/7$ (good solvent) or $\delta = 1/5$ (θ -solvent). Together with condition (5) this means that $N^\delta f l_B < b < N^{1-\nu} f l_B$. On the other hand, in the strong coupling case, $f l_B < b < N^\delta f l_B$, the forces necessary to induce a breakup of the structure are so strong that one is for $E \geq E_c$ already beyond the Pincus regime.

We note here that there are other systems in which strings and globules coexist: Especially polymers which are charged as a whole may take the form of necklaces; these may be ordered for uniformly charged polyelectrolytes in poor solvents⁵⁹ or disordered for random PAs with an excess charge $Q > Q_c$ ²². A coil-globule coexistence may also occur when a collapsed polymer in a poor solvent is deformed^{60,61}.

The instability at $E \cong E_c$ may be first order. Here we want to discuss a related, but distinct situation in which such a transition may be found: it concerns the deformation of a collapsed polymer in a poor solvent, as studied by Halperin and Zhulina⁶⁰. Similar to our case for weak deformations ΔL the response of the polymer is con-

trolled by the surface tension so that the restoring force f depends linearly on ΔL : $f \propto \Delta L$; this parallels Eq. (74) in the PA problem. On the other hand under strong deformations the chain breaks up in a series of equally sized (ideal) Pincus blobs, which again results in a linear relationship $f \propto \Delta L$; this corresponds in our problem to Eq. (58) (θ -solvent). For intermediate deformations Halperin and Zhulina find from a scaling analysis of a hypothetical cylindrical phase a $(\Delta L)^{-1/2}$ -dependence of f , i.e., they have a van der Waals-loop in the $(f, \Delta L)$ -diagram, which is reminiscent of a first-order transition. Using the Maxwell equal area construction⁴¹⁾ they postulate that in this regime $f \propto (\Delta L)^0$ and interpret this as a region where strings and globules coexist (for instance, a tadpole configuration).

In our case, however, a PA globule behaves differently under a slowly increasing field; this is due to the fact that the field strength E_D which is necessary to unravel the PA globule (by pulling a Debye blob out of the condensate in order to generate a string) is *much* higher than the critical value E_c (cf. Eq. (75)): E_D is given by $\sqrt{fg_D}qE_D r_D \approx T$ and thus $E_D/E_c \approx (N/g_D)^{1/2} r_D/R \gg 1$. Here the globule does not increase its size through discharging Debye blobs, but by a sudden breakup at $E \cong E_c \ll E_D$. This is different from the situation in ref.⁶⁰⁾ and it is due to the characteristic way in which the PA is coupled to the external field: The force acting on a portion of the chain containing g monomers scales typically with $g^{1/2}$ so that small parts of the chain prefer to remain in the condensate. Thus the surface tension controls the scenario (necklace forming) until a relatively high field $E \cong E_c$ is reached, at which the PA changes abruptly its state. We note that the surface-controlled scenario may be circumvented when the procedure is inverted, i.e., when one starts from the highly extended state and then decreases the field strength moderately. Then the PA may pass through coil-globule states (hysteresis effect). Another possibility to circumvent the surface-controlled scenario may be to start with a PA having a sufficiently high charge asymmetry so that the PA globule is already highly deformed in the absence of an external field. Being beyond the scope of this paper these effects deserve further investigation.

5. Dynamical properties

Here we study the dynamical properties of PAs in external electrical fields. We restrict our considerations to the weak coupling limit. The PA is modeled as in subsection 3.1 as a Gaussian chain. The dynamics is now incorporated via a Langevin-approach, i.e. one introduces Gaussian random forces which model the collisions of the solvent molecules with the monomers. As a first approximation we neglect the hydrodynamic interactions; this leads us to the exactly tractable Rouse model (cf. next subsection). Then we focus in subsection 5.2 on the hydrodynamic interaction which, as is known usually modifies the dynamics of polymers in dilute solutions drastically. As we show for small external fields this leads to the usual Zimm-dynamics, whereas a strongly deformed chain behaves like a rescaled Rouse chain, formed from Pincus blobs which now play the role of elementary units (“monomers”).

5.1. Rouse dynamics

As in section 3.1 we model the PA as a Gaussian chain consisting of N charged beads, connected by harmonic springs into a linear chain. In refs.^{35,36} we considered the dynamics of such a chain in terms of the Rouse model^{62,63} and we recall here the basic results. The chain's configuration is given by the set of vectors $\{\mathbf{R}_n(t)\}$, where $\mathbf{R}_n(t) = (X_n(t), Y_n(t), Z_n(t))$ is the position vector of the n th bead at time t ; $n = 0, 1, \dots, N-1$. The potential energy $U(\{\mathbf{R}_k(t)\})$ corresponds to the potential energy of the Gaussian chain, i.e., Eq. (10) (with $\mathbf{f} \equiv 0$) so that we have

$$U(\{\mathbf{R}_k(t)\}) = \frac{K}{2} \sum_{n=1}^{N-1} [\mathbf{R}_n(t) - \mathbf{R}_{n-1}(t)]^2 - \mathbf{E} \sum_{n=0}^{N-1} q_n \mathbf{R}_n(t) \quad (76)$$

The chain's dynamics is described by N coupled Langevin equations⁶³

$$\zeta \frac{\partial \mathbf{R}_n(t)}{\partial t} = - \frac{\partial U(\{\mathbf{R}_k(t)\})}{\partial \mathbf{R}_n(t)} + \mathbf{f}_R(n, t) \quad (77)$$

where the hydrodynamic interaction is disregarded. In Eq. (77) ζ is the friction constant and $\mathbf{f}_R(n, t)$ is the random thermal-noise force which mimics the collisions of the n th bead of the PA with the solvent molecules. The thermal noise is Gaussian with zero mean so that one has

$$\overline{f_i(n, t)} = 0, \quad \overline{f_i(n, t) f_j(n', t')} = 2\zeta T \delta_{ij} \delta_{nn'} \delta(t - t') \quad (78)$$

In Eq. (78) i and j denote the components of the force vector, i.e. $i, j = X, Y, Z$ and the dash stands for thermal averaging, i.e. averaging over the realizations of the Langevin forces $\mathbf{f}_R(n, t)$.

Regarding the suffix n as being continuous (i.e. considering the chain as an elastic string) and setting $\mathbf{E} = (0, E, 0)$ it follows from Eqs. (76) and (77)

$$\zeta \frac{\partial X_n(t)}{\partial t} = K \frac{\partial^2 X_n(t)}{\partial n^2} + f_X(n, t) \quad (79a)$$

$$\zeta \frac{\partial Z_n(t)}{\partial t} = K \frac{\partial^2 Z_n(t)}{\partial n^2} + f_Z(n, t) \quad (79b)$$

and

$$\zeta \frac{\partial Y_n(t)}{\partial t} = K \frac{\partial^2 Y_n(t)}{\partial n^2} + q_n E + f_Y(n, t) \quad (79c)$$

At the chain's ends one has the Rouse boundary conditions^{62,63}:

$$\left. \frac{\partial X_n(t)}{\partial n} \right|_{n=0, N} = \left. \frac{\partial Y_n(t)}{\partial n} \right|_{n=0, N} = \left. \frac{\partial Z_n(t)}{\partial n} \right|_{n=0, N} = 0 \quad (80)$$

Since the X - and Z -components of the \mathbf{R}_n are field-independent and follow the standard Rouse behavior^{62,63} we can restrict ourselves to the behavior of the Y -component, Eq. (79c). This equation contains two types of forces: the thermal noise term $f_Y(n, t)$ and a quenched force $q_n E$. We note that configuration-dependent forces were also considered recently in other cases based on the Rouse model, namely polymers in steady flows⁶⁴ and in random layered flows^{65,66}.

The solution of Eq. (79) with the boundary conditions, Eq. (80), is given in the form of a Fourier series⁶³

$$Y_n(t) = Y(0, t) + 2 \sum_{p=1}^{\infty} Y(p, t) \cos\left(\frac{p\pi n}{N}\right) \quad (81)$$

where $Y(p, t)$, $p = 0, 1, \dots$, denote the normal coordinates:

$$Y(p, t) = \frac{1}{N} \int_0^N dn \cos\left(\frac{p\pi n}{N}\right) Y_n(t) \quad (82)$$

In terms of the coordinates $Y(p, t)$ Eq. (79) can be rewritten as

$$\frac{\partial Y(p, t)}{\partial t} = -\frac{p^2}{\tau_R} Y(p, t) + \frac{1}{\zeta} \sigma_p E + \frac{1}{\zeta} \phi_Y(p, t) \quad (83)$$

Here τ_R is the *Rouse time*

$$\tau_R = \frac{\zeta b^2 N^2}{3\pi^2 T} \quad (84)$$

which is the longest internal relaxation time of the harmonic chain. The symbols σ_p and $\phi_Y(p, t)$ in Eq. (83) denote the Fourier transforms of the charge variable,

$$\sigma_p = \frac{1}{N} \int_0^N dn \cos\left(\frac{p\pi n}{N}\right) q_n \quad (85)$$

and of the thermal noises,

$$\phi_Y(p, t) = \frac{1}{N} \int_0^N dn \cos\left(\frac{p\pi n}{N}\right) f_Y(n, t) \quad (86)$$

respectively. From Eq. (78) the Fourier transformed forces follow:

$$\overline{\phi_Y(p, t)} = 0, \quad \overline{\phi_Y(p, t) \phi_Y(q, t')} = \frac{\zeta T}{N} (\delta_{pq} + \delta_{p0} \delta_{q0}) \delta(t - t') \quad (87)$$

We assume that the PA is at $t = 0$ in thermal equilibrium, i. e. that it has a Gaussian conformation. This can be accounted for automatically by stipulating the PA to have been subjected to the thermal forces since $t = -\infty$. Furthermore, switching on the electric field at $t = 0$, the normal coordinates are given by

$$Y(p, t) = \frac{1}{\zeta} \int_{-\infty}^t d\tau \varphi_Y(p, \tau) \exp(-p^2(t - \tau)/\tau_R) + \frac{\sigma_p E}{\zeta} \int_0^t d\tau \exp(-p^2(t - \tau)/\tau_R) \quad (88)$$

From Eqs. (81) and (88) we obtain now readily the explicit time dependence of the mean-square displacement (MSD) of the chain's CM, the mean squared end-to-end distance and the MSD of a tagged bead. We begin the analysis with the CM's motion. The Y -component of the trajectory of the CM is given by the 0th normal coordinate, i. e.,

$$Y_{CM}(t) = \frac{1}{N} \int_0^N dn Y_n(t) = Y(0, t) \quad (89)$$

Using Eq. (88) with $p = 0$ and the properties of $\varphi_Y(p, t)$, Eq. (87), we obtain the following general result for the MSD of the CM in the Y -direction:

$$\overline{\langle (Y_{CM}(t) - Y_{CM}(0))^2 \rangle} = \frac{2T}{\zeta N} t + \frac{E^2}{\zeta^2} \langle \sigma_0^2 \rangle t^2 \quad (90)$$

Note that the MSD of the CM contains two independent contributions: the conventional Rouse diffusion term^{62,63} which is proportional to t and a drift term due to the external electrical field proportional to t^2 . The drift results from the balance between the external force and the friction^{35,36}.

The Y -component of the end-to-end vector $\mathbf{P}(t)$, $P(t) = \mathbf{R}_N(t) - \mathbf{R}_0(t)$, follows from the Fourier series, Eq. (81), for $Y_0(t)$ and $Y_N(t)$:

$$P_Y(t) = Y_N(t) - Y_0(t) = -4 \sum_{\hat{p}} Y(p, t) \quad (91)$$

Here the hat on the right-hand side of Eq. (91) designates that the summation extends over odd, positive numbers only. Using Eqs. (87), (88) and (91) the mean-squared end-to-end distance follows^{35,36}

$$\overline{\langle P_Y^2(t) \rangle} = \frac{b^2 N}{3} + \frac{16 E^2}{\zeta^2} \sum_{\hat{p}} \sum_{\hat{q}} \langle \sigma_p \sigma_q \rangle \int_0^t d\tau_1 \int_0^t d\tau_2 \exp(-p^2 \tau_1 / \tau_R - q^2 \tau_2 / \tau_R) \quad (92)$$

Eq. (92) will be used below to calculate the short-time behavior $t \ll \tau_R$. The long-time behavior $t \gg \tau_R$, when the end-to-end distance has reached its equilibrium, obtains from Eq. (92) by evaluating the integrals:

$$\overline{\langle P_Y^2(\infty) \rangle} = \frac{b^2 N}{3} + \frac{16 E^2 b^4 N^4}{9 \pi^4 T^2} \sum_{\hat{p}} \sum_{\hat{q}} \frac{\langle \sigma_p \sigma_q \rangle}{p^2 q^2} \quad (93)$$

This result is identical to the corresponding expressions for the Gaussian chain, Eq. (17). This follows from the equivalence between $\int_0^N dk \tilde{Q}_k$ and $(4N^2/\pi^2) \sum_p \sigma_p/p^2$

The behavior of a tagged bead, say one of the chain's ends, is more complicated. Using Eq. (81) with $n = 0$, i. e.

$$Y_0(t) - Y_0(0) = Y(0, t) - Y(0, 0) + 2 \sum_{p=1}^{\infty} (Y(p, t) - Y(p, 0)) \quad (94)$$

together with Eqs. (87), (88) and (94) we obtain for the MSD of the 0th bead^{35,36}:

$$\begin{aligned} \overline{\langle (Y_0(t) - Y_0(0))^2 \rangle} &= \frac{4T}{\zeta N} \sum_{p=1}^{\infty} \int_0^t d\tau e^{-2p^2\tau/\tau_R} \\ &+ \frac{2T}{\zeta N} t + \frac{4E^2}{\zeta^2} t \sum_{p=1}^{\infty} \langle \sigma_0 \sigma_p \rangle \int_0^t d\tau e^{-p^2\tau/\tau_R} \\ &+ \frac{4E^2}{\zeta^2} \sum_{p=1}^{\infty} \sum_{q=1}^{\infty} \langle \sigma_q \sigma_p \rangle \int_0^t d\tau_1 \int_0^t d\tau_2 e^{-p^2\tau_1/\tau_R - q^2\tau_2/\tau_R} + \frac{E^2}{\zeta^2} \langle \sigma_0^2 \rangle t^2 \end{aligned} \quad (95)$$

Let us now investigate given charge patterns. As a simple example consider the situation in which only one bead of the polymer is charged, say one of its ends. Such a situation was realized experimentally by Perkins et al.⁶⁷⁻⁶⁹ and Wirtz⁷⁰ who dragged individual DNAs with optical tweezers or magnetic beads at one of their ends. There are some interesting features which connect the motion of singly charged polymers to other physical systems. In refs.^{35,71} we have shown that the dynamics of the charged bead is similar to the response of mechanical spring-dashpot arrangements under stress, a class of models which obeys fractional rheological constitutive equations (see ref.⁷² and references therein) and which we used for a mesoscopic picture of the sol-gel transition^{71,73}. Another related situation concerns the solid-on-solid description of wetting phenomena discussed by Abraham et al.⁷⁴. Here the spreading of a liquid drop on a solid substrate was examined using a Langevin equation approach similar to Eq. (79c).

In the case that only the head-bead of the polymer is charged the $\{q_n\}$ distribution obeys $q_n = q\delta_{n0}$ and the Fourier transformed σ_p , Eq. (85) has the form $\sigma_p = q/N$ for $p = 0, 1, 2, \dots$. Inserting this into Eq. (90) leads to

$$\overline{\langle (Y_{CM}(t) - Y_{CM}(0))^2 \rangle} = \frac{2T}{\zeta N} t + \frac{q^2 E^2}{\zeta^2 N^2} t^2 \quad (96)$$

The MSD of the CM contains two independent contributions: the conventional Rouse diffusion term proportional to t and a drift term due to the external field, proportional to t^2 . One can understand the N^{-2} -dependence of the drift term as follows: The electrical force acting on the chain, qE , is independent of N , whereas the friction is proportional to N . Under both forces the polymer moves ballistically, with a velocity $V \propto qE/\zeta N$.

From Eq. (92) we find the following short-time behavior $t \ll \tau_R$ for the Y -component of the end-to-end distance (see ref.³⁶⁾ for details):

$$\overline{P_Y^2(t)} = \frac{b^2 N}{3} + \frac{4q^2 E^2 b^2}{3\pi\zeta T} t \quad (97)$$

Thus $\overline{P_Y^2(t)}$ is the sum of two independent terms: the equilibrium end-to-end distance of a Rouse chain^{62,63)} (without external forces) and a term proportional to t as response to the external field. Using Eq. (93) we obtain for the equilibrium end-to-end distance at very long times, $t \gg \tau_R$:

$$\overline{P_Y^2(\infty)} = \frac{b^2 N}{3} + \frac{q^2 E^2 b^4 N^2}{36T^2} \quad (98)$$

The stretching of the chain in the Y -direction (the second term of Eq. (98)) is due to the charged bead pulled by the external field and is proportional to N^2 .

We now turn to the dynamics of the charged end of the chain. The short time behavior $t \ll \tau_R$ follows from Eq. (95) (see again ref.³⁶⁾ for details)

$$\overline{(Y_0(t) - Y_0(0))^2} = 4b\sqrt{\frac{T}{6\pi\zeta}} t^{1/2} + \frac{4q^2 E^2 b^2}{3\pi\zeta T} t \quad (99)$$

a result mentioned previously in ref.⁷⁵⁾ The first term in Eq. (99) shows a subdiffusive behavior (which also governs the short-time behavior of a bead in the absence of external forces) and can be interpreted as being induced by thermal processes, in which some local "defects", e.g., kinks, spread out diffusively along the length (bN) of the chain⁷⁶⁾. Since the chain's configuration in space is itself random-walk-like, so that in the absence of external forces $P_Y \propto bN^{1/2}$, these processes are spatially confined, which results in a subdiffusive behavior of single beads at short times. The second term describes the response of the charged monomer after switching on the electrical field E . This term is equal to the corresponding term of Eq. (97), which describes the short-time behavior of the end-to-end distance; the reason for this equality is that at short times the uncharged end of the chain is not affected by the external field. In the long-time regime, $t \gg \tau_R$, the bead's motion mirrors the motion of the CM of the chain. One finds from Eq. (95)³⁶⁾

$$\overline{(Y_0(t) - Y_0(0))^2} = \frac{2T}{\zeta N} t + \frac{q^2 E^2}{\zeta^2 N^2} t^2 \quad (100)$$

Let us turn now to the dynamics of random PAs^{35,36)}, for which the beads are either positively or negatively charged, $q_n = \pm q$; the distribution is such that different charges are uncorrelated, i. e. one has Eq. (9) which reads in the continuum limit $\langle q_n q_m \rangle = q^2 \delta(n - m)$. For the Fourier transformed charge variables we find now $\langle \sigma_0^2 \rangle = q^2/N$ and $\langle \sigma_p \sigma_r \rangle = (q^2/2N)\delta_{pr}$ otherwise.

Now we find from Eq. (90) for the MSD of the CM in the Y -direction:

$$\overline{\langle (Y_{CM}(t) - Y_{CM}(0))^2 \rangle} = \frac{2T}{\zeta N} t + \frac{q^2 E^2}{\zeta^2 N} t^2 \quad (101)$$

The drift term shows here a N^{-1} -dependence which is by a factor of N larger than in the case of one charged bead (cf. Eq. (96)). One can understand the N^{-1} -dependence of the drift term in the following way: due to the randomness of the q_n , the total charge of a chain is of the order of $N^{1/2}$. Hence the electric force acting on the chain goes as $N^{1/2}$, while the friction is proportional to N . Under both forces the CM moves ballistically, with a velocity $V \propto qE/\zeta\sqrt{N}$.

Consider now the behavior of the PA's end-to-end distance for a random placement of charges. From Eq. (92) we obtain the following short-time behavior ($t \ll \tau_R$):

$$\overline{\langle P_Y^2(t) \rangle} = \frac{b^2 N}{3} + \frac{16 b q^2 E^2 (\sqrt{2} - 1)}{3 \zeta^{3/2} \sqrt{3\pi T}} t^{3/2} \quad (102)$$

The response of the end-to-end distance to the electrical field follows a $t^{3/2}$ -behavior which mirrors the behavior of the chain's ends (see below). The equilibrium end-to-end distance ($t \gg \tau_R$) obeys

$$\overline{\langle P_Y^2(\infty) \rangle} = \frac{b^2 N}{3} + \frac{q^2 E^2 b^4 N^3}{108 T^2} \quad (103)$$

which recovers the result of the Gaussian chain, Eq. (31).

Now we turn to the dynamics of the PA's end. Making use of Eqs. (95) we obtain^{35,36)}

$$\overline{\langle (Y_0(t) - Y_0(0))^2 \rangle} = 4b \sqrt{\frac{T}{6\pi\zeta}} t^{1/2} + \frac{8 b q^2 E^2 (\sqrt{2} - 1)}{3 \zeta^{3/2} \sqrt{3\pi T}} t^{3/2} \quad (104)$$

for $t \ll \tau_R$. The $t^{3/2}$ -subdrift-term is by a factor 1/2 smaller than the corresponding term describing the short-time dynamics of the end-to-end distance, Eq. (102). For $t \gg \tau_R$ one has

$$\overline{\langle (Y_0(t) - Y_0(0))^2 \rangle} = \frac{2T}{\zeta N} t + \frac{q^2 E^2}{\zeta^2 N} t^2 \quad (105)$$

i. e. for long-times the bead follows the motion of the CM (cf. Eq. (101)).

The dynamics of PAs for a variety of additional charge patterns (alternating charges, polyelectrolytes, neutral random PAs, correlated distributions of charges) can be found in ref.³⁶⁾

We close our discussion of the Rouse model by noting that the PAs dynamics can also be derived using scaling arguments. Let us demonstrate this for the field-induced motion of a single bead in the case of PAs with random, long-range correlated sequences of charges^{19,47)}. For such sequences the net charge of the PA is given by $\langle Q_{tot}^2 \rangle \cong q^2 N^{2\gamma}$ with $0 \leq \gamma \leq 1$. The case $\gamma = 1/2$ corresponds to the uncorrelated case discussed above, whereas for $\gamma > 1/2$ the charges are positively and for $\gamma < 1/2$ negatively correlated. The extreme cases $\gamma = 1$ and $\gamma = 0$ correspond to polyelectrolytes and alternating PAs, respectively. Consider now a single bead. In the Rouse

picture, starting at $t = 0$, the total number g of neighboring monomers which are involved in a collective motion with this tagged bead grows for short times ($t \ll \tau_R$) as $g(t) = Ct^{1/2}$. When the Rouse time τ_R is reached, the PA moves as a whole, i.e. $g(\tau_R) \equiv N$, so that $C \equiv \sqrt{T}/(\sqrt{\zeta}b)$. Thus for short times, $t \ll \tau_R$, one finds:

$$g(t) \equiv \frac{\sqrt{T}}{\sqrt{\zeta}b} t^{1/2} \quad (106a)$$

whereas at longer times, $t \gg \tau_R$, one has

$$g(t) \equiv N \quad (106b)$$

The excess charge Q of the collectively moving set of beads grows with time; one has $\langle Q^2 \rangle \equiv q^2(g(t))^{2\gamma}$. The mobility of the set of beads decreases as $\mu \equiv (\zeta(g(t)))^{-1}$. The average velocity of the tagged monomer in the Y -direction, v_Y , is then given by the velocity of the collectively moving set around it. Thus it obeys $\langle v_Y^2(g) \rangle \equiv \mu^2 \langle Q^2 \rangle E^2 \equiv q^2 E^2 \zeta^{-2} g^{2\gamma-2}$ where g is given by Eq. (106a) for $t \ll \tau_R$ and by Eq. (106b) for $t \gg \tau_R$. The average displacement of a single bead can be estimated from the average displacement of the corresponding blob of g monomers, i.e. $\langle Y^2(t) \rangle \equiv \langle v_Y^2(g) \rangle t^2 \equiv q^2 E^2 \zeta^{-2} g^{2\gamma-2} t^2$. For $t \ll \tau_R$ one finds from Eq. (106a)

$$\langle Y^2(t) \rangle \equiv \frac{b^{2-2\gamma} q^2 E^2}{\zeta^{1+\gamma} T^{1-\zeta}} t^{1+\gamma} \quad (107)$$

For the uncorrelated case, $\gamma = 1/2$, this reproduces (up to a numerical constant of order 1) the field induced short-time behavior of the exact calculations, i.e. Eq. (104). For longer times the PA drifts as a whole and we find from Eq. (106b) $\langle Y^2(t) \rangle \equiv (q^2 E^2 / \zeta^2 N^{2-2\gamma}) t^2$ which corresponds for $\gamma = 1/2$ to Eq. (105). Note that for polyelectrolytes, $\gamma = 1$, the drift becomes independent of N ³⁶⁾ (see ref.⁷⁷⁾ for a detailed discussion of the mobility of polyelectrolytes).

5.2. Hydrodynamic interactions

In order to take the hydrodynamic interaction between the beads into account one has to extend Eq. (77). Introducing the mobility tensor \mathbf{H}_{nm} the corresponding Langevin equation has the form⁶³⁾

$$\frac{\partial \mathbf{R}_n(t)}{\partial t} = \sum_m \mathbf{H}_{nm} \cdot \left(-\frac{\partial U(\{\mathbf{R}_k(t)\})}{\partial \mathbf{R}_m(t)} + \mathbf{f}_R(m, t) \right) \quad (108)$$

where the moments of the Gaussian random force obey the known, suitable relations⁶³⁾. In the θ -case the potential energy U is given by Eq. (76), whereas in the good solvent case one has in addition the excluded volume contribution $U_1 = (1/2)vT \sum_{n,m} \delta(\mathbf{R}_n - \mathbf{R}_m)$, where v is the second virial coefficient. In the Rouse model the hydrodynamic interaction is disregarded and the mobility tensor is

diagonal, $\mathbf{H}_{nm} = \mathbf{I} \delta_{nm} / \zeta$ (with \mathbf{I} being the unit tensor, $I_{\alpha\beta} = \delta_{\alpha\beta}$), so that one recovers Eq. (77). Now the hydrodynamic interaction between the beads can be incorporated by using as the mobility matrix the *Oseen tensor*⁶³⁾

$$\mathbf{H}_{nm} = \frac{\mathbf{I}}{\zeta} \quad (109 \text{ a})$$

and

$$H_{nm} = \frac{1}{8\pi\eta_s |\mathbf{P}_{nm}|} (\mathbf{I} + \hat{\mathbf{P}}_{nm} \hat{\mathbf{P}}_{nm}) \quad \text{for } n \neq m \quad (109 \text{ b})$$

Here $\mathbf{P}_{nm} = \mathbf{R}_n - \mathbf{R}_m$, $\hat{\mathbf{P}}_{nm} = \mathbf{P}_{nm} / |\mathbf{P}_{nm}|$ and η_s denotes the viscosity of the solvent. Eq. (108) for $n = 0, 1, \dots, N-1$ with \mathbf{H}_{nm} given by Eq. (109) represent the equations of motion of the Zimm model^{63,78)} which is in agreement with experimental results on dilute polymer solutions.

Since the situation is now much more involved than in the Rouse case (subsection 5.1) we do not consider here the transient behavior which develops after switching on the external field. We thus investigate the PAs dynamics for the case that the external field E acts on the chain since $t = -\infty$, i. e. that, as in section 3, the chain is already in equilibrium. As usual we proceed by using the preaveraged Oseen tensor^{63,78)}, i. e. we replace \mathbf{H}_{nm} in Eq. (108) by $\bar{\mathbf{H}}_{nm}$, where the average is taken with respect to the PA's equilibrium distribution. Distinct from the original Zimm situation^{63,78)} where one has to average over the equilibrium distribution of the unperturbed Gaussian or excluded volume coils we have now to take this average with respect to the deformed states.

In order to simplify the averaging procedure we use the monoblock approximation (cf. subsection 3.3), i. e. we disregard the inhomogeneity of the stretching and assume all Pincus blobs to be of equal size. Thus we approximate the deformed state by a cigar-like shape; we assume that an effective force $F_{\text{eff}} = Q_{\text{eff}} E$ acts on both ends of the chain. The monoblock approximation becomes exact when only the end beads are charged and one has $F_{\text{eff}} \equiv F = qE$ (cf. Eq. (46)). For the other charge distributions discussed above one finds $F_{\text{eff}} \approx NqE$, i. e., $Q_{\text{eff}} \approx Nq$ for the SDP (see the discussion after Eq. (50)) and $F_{\text{eff}} \approx \sqrt{fN}qE$, i. e., $Q_{\text{eff}} \approx \sqrt{fN}q$ for randomly charged PAs (cf. the discussion after Eq. (58)).

Now we average the Oseen tensor with respect to the deformed state in the monoblock picture. Since in this approximation one has a homogeneous stretching of the chain the mean square distance between a given pair of monomers obeys

$$\overline{\mathbf{P}_{nm}^2} \approx b^2 |n - m|^{2\nu} + b^2 \left(\frac{bF_{\text{eff}}}{T} \right)^{2(1-\nu)/\nu} |n - m|^2 \quad (110)$$

(cf. Eq. (46)). This is consistent with the exact formula for the θ -case which is given in Eq. (22). From Eq. (110) we find two regimes for the distances between the beads, namely

$$\overline{P_{nm}} \approx \begin{cases} b |n-m|^{\nu} & \text{for } |n-m| \ll g_0 \\ b \left(\frac{bF_{eff}}{T} \right)^{(1-\nu)/\nu} |n-m| & \text{for } |n-m| \gg g_0 \end{cases} \quad (111)$$

where the crossover distance g_0 is given by $g_0 = (bF_{eff}/T)^{-1/\nu}$, i. e., by the number of monomers per Pincus blob. The preaveraging of the Oseen tensor is now performed by replacing in Eq. (109b) $1/P_{nm}$ by $1/\overline{P_{nm}} \approx 1/\overline{P_{nm}}$. Furthermore the average value of the tensor $\mathbf{I} + \hat{P}_{nm}\hat{P}_{nm}$ is given by $4/3 \mathbf{I}$ for $|n-m| \ll g_0$ ⁶³⁾ and by $\mathbf{I} + \hat{e}_Y\hat{e}_Y$ for $|n-m| \gg g_0$ (\hat{e}_Y being the unit vector in the Y -, i. e. in the field direction). Thus the preaveraged Oseen tensor is anisotropic for $|n-m| \gg g_0$. Neglecting this anisotropy (i. e., setting $\mathbf{I} + \hat{e}_Y\hat{e}_Y \approx \mathbf{I}$) \overline{H}_{nm} takes the form

$$\overline{H}_{nm} = h(n-m) \mathbf{I} \cong \begin{cases} \frac{\mathbf{I}}{\eta_s b |n-m|^{\nu}} & \text{for } |n-m| \ll g_0 \\ \frac{\mathbf{I}}{\eta_s b g_0^{\nu-1} |n-m|} & \text{for } |n-m| \gg g_0 \end{cases} \quad (112)$$

In terms of this tensor we arrive at the Langevin equation

$$\frac{\partial \mathbf{R}_n(t)}{\partial t} = \sum_m h(n-m) \left(-\frac{\partial U(\{\mathbf{R}_k(t)\})}{\partial \mathbf{R}_m(t)} + f_R(m, t) \right) \quad (113)$$

Especially in the θ -case, i. e., in the absence of excluded volume effects, the preaveraging procedure leads to linear equations for the \mathbf{R}_n and decouples the X -, Y - and Z -components.

Following now ref.⁶³⁾ we transform Eq. (113) to the Rouse normal coordinates, as defined in Eq. (82). This leads to

$$\frac{\partial \mathbf{R}(p, t)}{\partial t} = \sum_q h_{pq} (-K_q \mathbf{R}(q, t) + \sigma_q \mathbf{E} + \varphi_R(q, t)) \quad (114)$$

where σ_p and φ_R are defined in Eqs. (85) and (86). Moreover h_{pq} obeys

$$h_{pq} = \frac{2 - \delta_{q0}}{N} \int_0^N dn \int_0^N dm \cos\left(\frac{p\pi n}{N}\right) \cos\left(\frac{p\pi m}{N}\right) h(n-m) \quad (115)$$

and can be calculated similarly to ref.⁶³⁾ (cf. Eqs. (4.53)–(4.56) therein). Thus we find that h_{pq} is approximately given by

$$h_{pq} \cong \left[\frac{N^{1-\nu}}{q^{1-\nu} \eta_s b} \int_0^{\frac{q\pi g_0}{N}} dx \frac{\cos x}{x^{\nu}} + \frac{1}{\eta_s b g_0^{\nu-1}} \int_{\frac{q\pi g_0}{N}}^{\infty} dx \frac{\cos x}{x} \right] \delta_{pq} \quad (116)$$

i. e., despite of the hydrodynamic interactions the Rouse normal coordinates are nearly decoupled. Now Eq. (116) can be approximated by

$$h_{pq} \equiv \begin{cases} \frac{1}{\eta_s b g_0^{v-1}} \ln\left(\frac{N}{g_0 \pi p}\right) \delta_{pq} & \text{for } 0 < p \ll \frac{N}{g_0} \\ \frac{1}{\eta_s b N^{v-1}} p^{v-1} \delta_{pq} & \text{for } p \gg \frac{N}{g_0} \end{cases} \quad (117)$$

Furthermore h_{00} is calculated separately using Eq. (115) giving

$$h_{00} \equiv \begin{cases} \frac{1}{\eta_s b g_0^{v-1}} \ln(N/g_0) & \text{for } g_0 \ll N \\ 1/(\eta_s b N^{v-1}) & \text{for } g_0 \gg N \end{cases} \quad (118)$$

In Eq. (114) K_p follows directly in the θ -case to be $K_p = 3\pi^2(T/b^2)(p/N)^2$. In the case of a good solvent the linear form of Eq. (114) is an approximation⁶³⁾. The strategy here is to choose the K_p such that the distribution of the $\mathbf{R}(p, t)$ is consistent with the properties of the equilibrium conformation, Eq. (111). The behavior for short distances, $|n - m| \ll g_0$, corresponds to large p , $p \gg N/g_0$. Following now the procedure described in section 4.2.2 in ref.⁶³⁾ one finds $K_p \equiv (T/b^2)(p/N)^{2v+1}$ for $p \gg N/g_0$. On the other hand the K_p for $p \ll N/g_0$ follow from the requirement that the thermally averaged equilibrium solutions of Eq. (114), i.e. $\overline{Y(p, t)} = \int_{-\infty}^t d\tau e^{-K_p(t-\tau)/\zeta_p} (\sigma_p/\zeta_p) E = (\sigma_p/K_p) E = ((-1)^p - 1) F_{\text{eff}}/(NK_p)$ with $\zeta_p = 1/h_{pp}$, lead to the homogeneous stretching of the PA (cf. Eq. (111) for $|n - m| \gg N/g_0$), i.e. $\overline{Y(p, t)} \equiv ((-1)^p - 1) b g_0^{v-1} N/p^2$. Thus we find:

$$K_p \equiv \begin{cases} \frac{T}{b^2 g_0^{2v-1} N^2} p^2 & \text{for } p \ll N/g_0 \\ \frac{T}{b^2 N^{2v+1}} p^{2v+1} & \text{for } p \gg N/g_0 \end{cases} \quad (119)$$

Now it can be seen from Eqs. (117) and (119) that the behavior for large p , $p \gg N/g_0$, is the usual Zimm behavior described by the Langevin equation⁶³⁾

$$\frac{\partial \mathbf{R}(p, t)}{\partial t} = -\frac{p^{3v}}{\tau_r} \mathbf{R}(p, t) + \frac{1}{\zeta_p} \sigma_p \mathbf{E} + \frac{1}{\zeta_p} \varphi_R(p, t) \quad (120)$$

Here $\tau_r \equiv \eta_s b^3 N^{3v}/T$ is the rotational relaxation time of the unperturbed Zimm chain⁶³⁾. On the other hand neglecting the logarithmic factors in Eqs. (117) and (118) we find for $p \ll N/g_0$ that $h_{pp} = \zeta_p^{-1} = g_0/\zeta$ is p -independent. Thus for small p , $p \ll N/g_0$, the Langevin equation (for the Y -direction) obeys

$$\frac{\partial \mathbf{R}(p, t)}{\partial t} = \frac{K_p g_0}{\zeta} \mathbf{R}(p, t) \frac{g_0}{\zeta} \sigma_p \mathbf{E} + \frac{g_0}{\zeta} \varphi_R(p, t) \quad (121)$$

Setting $K_p g_0 / \tilde{\zeta} = p^2 / \tilde{\tau}_R$ with

$$\tilde{\tau}_R \equiv \frac{\tilde{\zeta} b^2 g_0^{2\nu-2} N^2}{T} \quad (122)$$

it can be seen that for $p \ll N/g_0$ one has a rescaled Rouse behavior, where the Rouse time is given now by Eq. (122).

These results for the dynamics of stretched polymer chains were already derived by Pincus⁷⁹⁾ using a slightly different approach. In ref.⁷⁹⁾ these results are also interpreted in terms of Pincus blobs. As discussed in section 3.3 the homogeneously stretched chain (or an inhomogeneously stretched chain in the monoblock approximation) can be described as a string of blobs of size $\xi = T/F_{eff}$ consisting of $g_0 = (\xi/b)^{1/\nu}$ monomers. Inside the blobs there is an unscreened hydrodynamic coupling between the monomers. Thus the PA's dynamics for length scales smaller than ξ , i.e., for $p \gg N/g_0$, are described by the usual Zimm model, Eq. (120). For length scales larger than ξ , i.e., for $p \ll N/g_0$, the stretched polymer behaves like a Rouse chain. The renormalized units are the N/g_0 blobs, each having the friction constant of Stokes sphere, $\tilde{\zeta} \equiv \eta_s \xi$, and a "spring constant" of $\tilde{K} \equiv T/\xi^2$ (cf. Eq. (45) with $N = g_0$). Thus the Rouse time is given by $\tilde{\tau}_R \equiv \tilde{\zeta} \xi^2 (N/g_0)^2 / T$ so that one recovers Eq. (122).

Thus we have found that the PA's dynamics shows two characteristic regimes which depend on the strength of the external fields. When E is sufficiently small so that $g_0 \gg N$, i.e., $E \ll T/(Q_{eff} b N^\nu)$, the equilibrium conformation is only weakly perturbed and one has for all modes the ordinary Zimm dynamics, Eq. (120). If the external field is strong enough so that one has $g_0 \ll N$, i.e. $E \gg T/(Q_{eff} b N^\nu)$, the PA behaves effectively as a Rouse chain. For the dependence of the rotational relaxation time $\tau_r = \zeta_l / K_l$ on the external field E follows:

$$\tau_r \equiv \begin{cases} \frac{\eta_s b^3 N^{3\nu}}{T} & \text{for } E \ll T/(Q_{eff} b N^\nu) \\ \frac{\eta_s b^{2/\nu} N^2 Q_{eff}^{(2-3\nu)/\nu}}{T^{(2-2\nu)/\nu}} E^{(2-3\nu)/\nu} & \text{for } E \gg T/(Q_{eff} b N^\nu) \end{cases} \quad (123)$$

i.e., when the external field increases the dynamics is effectively slowed down. A similar effect occurs for the self diffusion constant of the CM⁶³⁾, $D_G = T/(N\zeta_0)$, which obeys

$$D_G \equiv \begin{cases} \frac{T}{\eta_s b N^\nu} & \text{for } E \ll T/(Q_{eff} b N^\nu) \\ \frac{T^{1/\nu} Q_{eff}^{(\nu-1)/\nu}}{\eta_s b^{1/\nu} N} E^{(\nu-1)/\nu} & \text{for } E \gg T/(Q_{eff} b N^\nu) \end{cases} \quad (124)$$

Another possibility to observe the dynamics of the PA may be to superimpose on the external field E a small oscillatory field $E_\omega(t) = E_\omega e^{i\omega t}$ with $E_\omega \ll E$. Now the

response of the stretched PA to this perturbation follows from the considerations of subsection 5.1. In the monoblock picture the charge distributions of the Pincus blobs is given by $\{q_{\tilde{n}}^{(P)}\}$ with $q_{\tilde{n}}^{(P)}$ being the charge of the \tilde{n} th Pincus blob ($\tilde{n} = 0, \dots, N/g_0$). The end-to-end distance $P_Y(t)$ oscillates around the unperturbed end-to-end distance P_Y (i. e., the distance for $E_\omega = 0$) as follows (cf. Eq. (91)):

$$\overline{P_Y(t) - P_Y} \cong - \frac{E_\omega}{\zeta} \sum_p \sigma_p^{(P)} \int_{-\infty}^t d\tau e^{i\omega\tau} e^{-p^2(t-\tau)/\tau_R} \quad (125)$$

Especially for a PA with oppositely charged ends, i. e., $q_0^{(P)} = -q$, $q_{N/g_0}^{(P)} = q$ and $q_{\tilde{n}}^{(P)} = 0$ otherwise one has $\sigma_p^{(P)} = ((-1)^p - 1)q/(N/g_0)$. This results in

$$\overline{P_Y(t) - P_Y} \cong - \frac{q}{\sqrt{\zeta \bar{K}}} (\i\omega)^{-1/2} E_\omega(t) \quad (126)$$

as long as $\omega\tau_R \gg 1$, a result which we already discussed for the ordinary Rouse model^{35,71}. This means that one has (independently of frequency) a phase angle $\pi/4$ between the oscillations of the field and the response of the conformation.

In this section our considerations were based up-to-now on the monoblock approximation, where all Pincus blobs have the same size. As discussed in subsection 3.3 one encounters in general a string of Pincus blobs of different sizes $\zeta_{\tilde{n}}$, with $\tilde{n} = 1, \dots, N/g_0$. Thus the PA may be viewed as an inhomogeneous Rouse chain where the rigidity of the ‘‘springs’’ and the friction constants of the ‘‘beads’’ vary along the arclength of the chain, namely $\bar{K}_{\tilde{n}} \cong T/\zeta_{\tilde{n}}^2$ and $\zeta_{\tilde{n}} \cong \eta_s \xi_{\tilde{n}}$. Taking such an inhomogeneity into account Marciano and Brochard-Wyart⁸⁰ have determined the normal modes of a tethered polymer in a strong flow (trumpet). They show that the modes are given by zero-order Bessel functions, but which (in a good approximation) lead again to the mode spectrum of the homogeneous Rouse chain. In ref.⁸⁰ the authors find for a small oscillatory force applied at the free end a relation similar to Eq. (126) (the oscillatory force may be realized by applying a magnetic field to a tethered DNA with a magnetic bead on its free end). In ref.⁸¹ we have calculated the response of an inhomogeneous ladder model to an applied force (this problem can be mapped directly on the Rouse chain³⁵). We showed that by a suitable choice of spring constants and viscosities one can attain more complex relations between force and deformation than the one given in Eq. (126); in particular the constant phase angle can lie anywhere within the interval from 0 to $\pi/2$. Thus the interesting question arises whether by a suitably chosen charge distribution the dynamics of stretched PAs may also show such a generalized behavior; this deserves further investigations which are now in progress.

6. Conclusion

In this work we have considered conformational and dynamical properties of PAs in external electrical fields. The electrostatic interaction between the charged monomers gives rise to different characteristic regimes, namely that the global electro-

static free energy is small or large compared to the thermal energy T (weak coupling limit or strong coupling case). We have considered here both regimes separately. In the weak coupling limit we have started by calculating analytically conformational properties of Gaussian chains. Then we have taken care of the finite extensibility of the polymer by modeling the PA as a freely-jointed chain. The role of the excluded volume was estimated in terms of a scaling approach: As we have shown, stretched PAs can be described by strings of Pincus blobs of different sizes where the PAs' overall geometry is determined by their charge distribution. In the strong coupling case we studied PAs' conformational properties and showed that PAs with a vanishing total charge collapse into spherical globules. Here the response of the PA to not-too-strong electrical fields is determined by the competition of the external perturbation and the surface tension. We predict an instability at a critical external field E_c , above which the PA lengthens rapidly. Finally, we have investigated the dynamics of PAs in the weak coupling limit. In terms of the Rouse model the dynamics can be calculated exactly. We further studied the role of hydrodynamic interactions and found that with increasing field-strength one has a crossover from the Zimm- to the Rouse-dynamics.

The authors are indebted to Dr. G. Oshanin and Dr. J.-U. Sommer for fruitful discussions. Financial support by the EC grant CHRX-CT93-0354, by the Deutsche Forschungsgemeinschaft and by the Fonds der Chemischen Industrie is gratefully acknowledged.

- 1) T. E. Creighton, "Proteins: Their Structure and Molecular Properties", Freeman, San Francisco 1984
- 2) T. Garel, H. Orland, *Europhys. Lett.* **6**, 307 (1988)
- 3) E. I. Shakhnovich, A. M. Gutin, *J. Phys. A* **22**, 1647 (1989)
- 4) K. A. Dill, S. Bromberg, K. Yue, K. M. Fiebig, D. P. Yee, D. P. Yee, P. D. Thomas, H. S. Chan, *Protein Sci.* **4**, 561 (1995)
- 5) E. Shakhnovich, V. Abkevich, O. Ptitsyn, *Nature (London)* **379**, 96 (1996)
- 6) M. Mezard, G. Parisi, M. A. Virasoro, "Spin Glass Theory and Beyond", World Scientific, Singapore 1987
- 7) K. Binder, A. P. Young, *Rev. Mod. Phys.* **58**, 801 (1986)
- 8) S. F. Edwards, P. R. King, P. Pincus, *Ferroelectrics* **30**, 3 (1980)
- 9) C. Qian, A. L. Kholodenko, *J. Chem. Phys.* **89**, 5273 (1988)
- 10) V. Yu. Borue, I. Ya. Erukhimovich, *Macromolecules* **23**, 3625 (1990)
- 11) Y. Kantor, M. Kardar, *Europhys. Lett.* **14**, 421 (1991)
- 12) P. G. Higgs, J. F. Joanny, *J. Chem. Phys.* **94**, 1543 (1991)
- 13) P. G. Higgs, H. Orland, *J. Chem. Phys.* **95**, 4506 (1991)
- 14) Y. Kantor, H. Li, M. Kardar, *Phys. Rev. Lett.* **69**, 61 (1992)
- 15) M. Schulz, S. Stepanow, *J. Chem. Phys.* **98**, 5074 (1993)
- 16) J. M. Victor, J. B. Imbert, *Europhys. Lett.* **24**, 189 (1993)
- 17) Y. Kantor, M. Kardar, H. Li, *Phys. Rev. E* **49**, 1383 (1994)
- 18) J. Wittmer, A. Johnner, J. F. Joanny, *Europhys. Lett.* **24**, 263 (1993)
- 19) A. M. Gutin, E. I. Shakhnovich, *Phys. Rev. E* **50**, R3322 (1994)
- 20) Y. Kantor, M. Kardar, *Europhys. Lett.* **27**, 643 (1994)

- 21) A. V. Dobrynin, M. Rubinstein, *J. Phys. II (France)* **5**, 677 (1995)
- 22) Y. Kantor, M. Kardar, *Phys. Rev. E* **51**, 1299 (1995)
- 23) Y. Kantor, M. Kardar, *Phys. Rev. E* **52**, 835 (1995)
- 24) Y. Levin, M. C. Barbosa, *Europhys. Lett.* **31**, 513 (1995)
- 25) D. Ertas, Y. Kantor, *Phys. Rev. E* **53**, 846 (1996)
- 26) D. Srivastava, M. Muthukumar, *Macromolecules* **29**, 2324 (1996)
- 27) C. L. McCormick, C. B. Johnson, *Macromolecules* **21**, 694 (1988)
- 28) J.-M. Corpart, F. Candau, *Macromolecules* **26**, 1333 (1993)
- 29) M. Skouri, J. P. Munch, S. J. Candau, S. Neyret, F. Candau, *Macromolecules* **27**, 69 (1994)
- 30) M. Annaka, T. Tanaka, *Nature (London)* **355**, 430 (1992)
- 31) X. Yu, A. Tanaka, K. Tanaka, T. Tanaka, *J. Chem. Phys.* **97**, 7805 (1992)
- 32) J. P. Baker, H. W. Blanch, J. M. Prausnitz, *Polymer* **36**, 1061 (1995)
- 33) A. E. English, S. Mafé, J. A. Manzanares, X. Yu, A. Y. Grosberg, T. Tanaka, *J. Chem. Phys.* **104**, 8713 (1996)
- 34) H. Schiessel, A. Blumen, *J. Chem. Phys.* **105**, 4250 (1996)
- 35) H. Schiessel, G. Oshanin, A. Blumen, *J. Chem. Phys.* **103**, 5070 (1995)
- 36) H. Schiessel, G. Oshanin, A. Blumen, *Macromol. Theory Simul.* **5**, 45 (1996)
- 37) H. Schiessel, A. Blumen, *J. Chem. Phys.* **104**, 6036 (1996)
- 38) J.-U. Sommer, M. Daoud, *Phys. Rev. E* **53**, 905 (1996)
- 39) K. Binder, *J. Chem. Phys.* **79**, 6387 (1983)
- 40) U. K. Chaturvedi, U. Steiner, O. Zak, G. Krausch, J. Klein, *Phys. Rev. Lett.* **63**, 616 (1989)
- 41) L. D. Landau, E. M. Lifshitz, "Statistical Physics", Pergamon, New York 1981
- 42) J. des Cloizeaux, *J. Phys. (Paris)* **36**, 281 (1975)
- 43) P. G. de Gennes, "Scaling Concepts in Polymer Physics", Cornell Univ. Press, Ithaca 1979
- 44) S. Neyret, A. Baudouin, J. M. Corpart, F. Candau, *Nuovo Cimento D* **16**, 669 (1994)
- 45) A. Yu. Grosberg, A. R. Khokhlov, "Statistical Physics of Macromolecules", AIP Press, New York 1994
- 46) P. Pfeuty, R. M. Velasco, P. G. de Gennes, *J. Phys. (Paris) Lett.* **38**, L5 (1977)
- 47) C.-K. Peng, S. V. Buldyrev, A. L. Goldberger, S. Havlin, F. Sciortino, M. Simons, H. E. Stanley, *Nature (London)* **356**, 168 (1992)
- 48) J.-U. Sommer, A. Blumen, *J. Phys. A* **28**, 6669 (1995)
- 49) S. Havlin, A. Bunde, in "Fractals and Disordered Systems", A. Bunde, S. Havlin, Eds., Springer, Berlin 1991, p. 97 ff.
- 50) P. J. Flory, "Statistical Mechanics of Chain Molecules", Interscience, New York 1969
- 51) R. K. Pathria, "Statistical Mechanics", Pergamon Press, Oxford 1972
- 52) W. Feller, "An Introduction to Probability Theory and Its Applications" Vol. I, Wiley, New York 1968
- 53) P. Pincus, *Macromolecules* **9**, 386 (1976)
- 54) F. Brochard-Wyart, *Europhys. Lett.* **23**, 105 (1993)
- 55) F. Brochard-Wyart, *Europhys. Lett.* **30**, 387 (1995)
- 56) J. Spanier, K. B. Oldham, "An Atlas of Functions", Hemisphere, Washington 1987
- 57) F. Brochard-Wyart, H. Hervet, P. Pincus, *Europhys. Lett.* **26**, 511 (1994)
- 58) J. D. Sherwood, *J. Fluid Mech.* **188**, 133 (1988)
- 59) A. V. Dobrynin, M. Rubinstein, S. P. Obukhov, *Macromolecules* **29**, 2974 (1996)
- 60) A. Halperin, E. B. Zhulina, *Europhys. Lett.* **15**, 417 (1991)
- 61) M. Wittkop, S. Kreitmeier, D. Göritz, *Phys. Rev. E* **53**, 838 (1996)
- 62) P. E. Rouse, *J. Chem. Phys.* **21**, 1272 (1953)
- 63) M. Doi, S. F. Edwards, "The Theory of Polymer Dynamics", Oxford Univ. Press, Oxford 1986

- 64) W. Carl, *Macromol. Theory Simul.* **5**, 1 (1996)
- 65) G. Oshanin, A. Blumen, *Phys. Rev. E* **49**, 4185 (1994)
- 66) G. Oshanin, A. Blumen, *Macromol. Theory Simul.* **4**, 87 (1995)
- 67) T. T. Perkins, D. E. Smith, S. Chu, *Science (Washington, D.C.)* **264**, 819 (1994)
- 68) T. T. Perkins, S. R. Quake, D. E. Smith, S. Chu, *Science (Washington, D.C.)* **264**, 822 (1994)
- 69) T. T. Perkins, D. E. Smith, R. G. Larson, S. Chu, *Science (Washington, D.C.)* **268**, 83 (1995)
- 70) D. Wirtz, *Phys. Rev. Lett.* **75**, 2436 (1995)
- 71) H. Schiessel, A. Blumen, *Fractals* **3**, 483 (1995)
- 72) H. Schiessel, R. Metzler, A. Blumen, T. F. Nonnenmacher, *J. Phys. A* **28**, 6567 (1995)
- 73) H. Schiessel, A. Blumen, *Macromolecules* **28**, 4013 (1995)
- 74) D. Abraham, P. Collet, J. De Coninck, F. Dunlop, *J. Stat. Phys.* **61**, 509 (1990)
- 75) S. F. Burlatsky, G. S. Oshanin, A. V. Mogutov, M. Moreau, *Phys. Lett. A* **166**, 230 (1992)
- 76) P. G. de Gennes, *J. Chem. Phys.* **55**, 572 (1971)
- 77) M. Muthukumar, *Macromol. Theory Simul.* **3**, 61 (1994)
- 78) B. H. Zimm, *J. Chem. Phys.* **24**, 269 (1956)
- 79) P. Pincus, *Macromolecules* **10**, 210 (1977)
- 80) Y. Marciano, F. Brochard-Wyart, *Macromolecules* **28**, 985 (1995)
- 81) H. Schiessel, A. Blumen, *J. Phys. A* **26**, 5057 (1993)